

Correlation between Gross Motor Function and MRI Brain Morphology in Children with Cerebral Palsy

Maesa Al Hallak

Aus der Kinderklinik und Kinderpoliklinik im Dr. von Haunerschen
Kinderspital
Klinik der Ludwig-Maximilians-Universität München
Vorstand: Prof. Dr. med. Dr. sci. nat. C. Klein

Correlation between Gross Motor Function and MRI Brain Morphology in Children with Cerebral Palsy

Dissertation
zum Erwerb des Doktorgrades der Medizin
an der Medizinischen Fakultät der
Ludwig-Maximilians-Universität zu München

vorgelegt von
Maesa Al Hallak

aus Damaskus
2018

Mit Genehmigung der Medizinischen Fakultät
der Universität München

Berichterstatter: Prof. Dr. med. Florian Heinen

Mitberichterstatter: PD Dr. Christoph Lücking

Mitbetreuung durch die
promovierten Mitarbeiter: Prof. Dr. med. Birgit Ertl-Wagner
PD Dr. med. Sebastian Schröder

Dekan: Prof. Dr. med. dent. Reinhard Hickel

Tag der mündlichen Prüfung: 12.04.2018

For my lovely Damascus,
the City of Jasmine

CONTENTS

1	Introduction	9
1.1	Cerebral Palsy	9
1.1.1	Definition of Cerebral Palsy	9
1.1.2	Epidemiology	9
1.1.3	Etiology	10
1.1.4	Classification of Cerebral Palsy	11
1.1.4.1	Subtypes of Cerebral Palsy	11
1.1.4.2	Severity of Cerebral Palsy according to GMFCS	12
1.2	Periventricular Leukomalacia	14
1.2.1	Definition of Periventricular Leukomalacia	14
1.2.2	Pathology of Periventricular Leukomalacia	14
1.2.3	Pathophysiology of Periventricular Leukomalacia	17
1.3	The Role of Imaging in PVL	18
1.3.1	The Role of Ultrasound in PVL	18
1.3.2	The Role of MRI in PVL	19
1.4	Previous Clinical Studies	21
2	Aim of the Study	22
3	Methods	22
3.1	Study Design	22
3.2	Subjects	23
3.3	MRI-Protocol	24
3.4	Statistical Analysis	29
4	Result	29
4.1	Total Cohort Characteristics	29
4.2	Subgroup Data of Patients according to GMFCS	31
4.2.1	Correlation between GMFCS Level and gestational age at birth	32
4.2.2	Correlation between GMFCS Level and age at MRI-examination	32
4.2.3	Correlation between GMFCS Level and MRI-findings	33
4.2.3.1	Study of Corpus Callosum	33
4.2.3.1.1	Study of length of corpus callosum	33
4.2.3.1.2	Study of genu of corpus callosum	34
4.2.3.1.3	Study of thickness of thinnest part of corpus callosum	35
4.2.3.1.4	Study of location of thinnest part of corpus callosum	36
4.2.3.1.5	Study of correlation between all parameters of corpus callosum	38
4.2.3.2	Study of Brainstem	39
4.2.3.2.1	Study of Midbrain	39
4.2.3.2.2	Study of Cerebral Peduncles	41
4.2.3.2.3	Study of Pons	42
4.2.3.3	Study of Lateral Ventricles	43

	4.2.3.3.1	Study of grade of extension of lateral ventricles	43
	4.2.3.3.2	Study of width of posterior horn of lateral ventricles	44
	4.2.3.3.3	Study of depth of extraction of lateral ventricles	45
	4.2.3.3.4	Study of distance between lateral ventricle and cortex	46
	4.2.3.3.5	Study of distance between extraction of lateral ventricle and cortex	47
	4.2.3.4	Study of gliosis	48
	4.2.3.4.1	Study of grade of gliosis	48
	4.2.3.4.2	Study of width of gliosis	48
	4.2.3.4.3	Study of the distance between gliosis and cortex	49
	4.2.3.5	Small Porencephalic Cysts in MRI "black holes"	50
	4.2.3.6	Microhemorrhage on T2*-weighted gradient echo MRI	51
	4.2.4	Correlation between left and right of MRI-findings	52
4.3		Subgroup Data of Patients according to gestational age	53
	4.3.1	Correlation between gestational age and MRI-findings	53
	4.3.1.1	Study of Corpus Callosum	53
	4.3.1.2	Study of Brainstem	53
	4.3.1.3	Study of Lateral Ventricles	54
	4.3.1.4	Study of Gliosis	54
	4.3.1.5	Small Porencephalic Cysts in MRI "black holes"	54
	4.3.1.6	Microhemorrhage on T2*-weighted gradient echo MRI	54
5		Discussion	56
	5.1	Total cohort	56
	5.2	GMFCS Level and MRI-findings	57
	5.3	Gestational age	60
6		Conclusion	62
7		References	64
8		List of Figures	68
9		List of Tables	70
10		List of Abbreviations	72
11		Appendix	73
12		Thanks	74

1 Introduction

1.1 Cerebral Palsy

Cerebral palsy is the most common cause of spastic movement disorders in children^(1,2). Our understanding of the etiology of the disease has been greatly advanced by the development of magnetic resonance imaging (MRI), which allows the identification of the underlying structural changes in the brain^(5, 6), giving information on topography as well as the extent and potential timing of the causative lesion^(7, 8, 9).

1.1.1 Definition of Cerebral Palsy:

Cerebral palsy (CP) describes a group of disorders of the development of movement and posture, causing impaired function, due to non-progressive disturbances occurs in the developing fetal or infant brain. The motor disorders are often accompanied by disturbances of cognition, communication, perception, behaviour and epilepsy⁽¹⁰⁾.

1.1.2 Epidemiology:

Cerebral palsy (CP) is the most prevalent cause of motor disorder in childhood⁽¹⁰⁾. The incidence of CP is about 2 per 1000 live births⁽¹¹⁾. The prevalence increases with lower birth weight and higher immaturity⁽¹¹⁾. Studies of the patterns of cerebral palsy in relation to birth weight show that very low birth weight (VLBW) newborns, i.e., weighing less than 1500 grams, are between 20 and 80 times more likely to have cerebral palsy than newborns with a birth weight of more than 2500 grams⁽¹¹⁾. Epidemiologic data has shown that with the advanced care in neonatal medicine, the incidence and severity of CP in premature VLBW newborns in Europe⁽³⁾ and northern America⁽⁴⁾ is decreasing. The majority of children affected with CP survive into adulthood, but life expectancy is negatively affected by the presence of severe function impairment and retardation⁽¹⁴⁾.

1.1.3 Etiology:

Cerebral palsy is caused by a wide spectrum of developmental and acquired abnormalities of the immature brain⁽²⁷⁾. The etiology of CP is extensive, ranging from prenatal and perinatal events to postnatal insults^(15, 16, 17, 18, 19). The pattern of brain lesions that leads to CP depends on the stage of brain development⁽⁸⁾. Cortical neurogenesis and brain lesions which are characterized by maldevelopment of the brain; they predominantly take place⁽⁸⁾ during the first and second trimester. During the early 3rd trimester, periventricular white matter is especially affected. Toward the end of the 3rd trimester, gray matter appears to be more vulnerable, whether it is a cortical or deep gray matter, such as ganglia and thalamus. During the first and second trimester, patterns develop usually in utero, whereas at the third trimester the lesions can be acquired in or ex utero⁽²⁵⁾. These different patterns are indicated in (Tab.1).

Even after neuroimaging and metabolic investigation, CP remains without identification or clear etiology in around 15% of children⁽¹⁴⁾.

Tab. 1. Pattern of brain lesions relative to the stage of brain development ⁽⁸⁾ .		
1st+2 nd trimester	3rd trimester	lesion
Maldevelopment		
Disorders of migration	Early/mid 3rd trimester	White
Lissencephaly		matter
Pachygyria	Intracranial hemorrhage	
Heterotopias	Periventricular leukomalacia	
	Periventricular infarction	
	Thromboembolic lesions	
	Multicystic encephalomalacia	
Disorders of proliferation	Late 3rd trimester	Gray
Hemimegalencephaly		matter
Cortical dysplasia	Basal ganglia/thalamus lesions	
Disorders of organization	Cortico-subcortical lesion	
Schizencephaly	Thromboembolic lesions	
Polymicrogyria	Multicystic encephalomalacia	
Hydranencephaly		
Anencephaly		

1.1.4 Classification of Cerebral Palsy:

1.1.4.1 Subtypes of Cerebral Palsy:

Cerebral palsy is usually evident in the first 12 to 18 months of life. The early indicators of the presence of motor disability include: delay in the appearance of the motor milestones, exaggerated or persistent primitive reflexes^(14, 19, 20), early hand preference, asymmetric motor function and abnormalities of muscle tone⁽¹⁴⁾. Cerebral palsy, according to European classification, can be divided into four major types (Tab.2): spastic (bilateral or unilateral) 50%, dyskinetic (dystonic or chorea-athetotic) 20%, ataxic 10% and mixed 20%^(14, 22). Serial neurodevelopmental evaluations are often required for proper classification of the subtype.

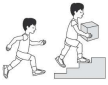
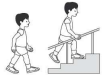



Tab. 2. Classification of cerebral palsy ⁽¹¹⁾ .
Spastic type: Spastic CP is characterized by at least two of the following: <ul style="list-style-type: none">• Abnormal pattern of posture and/or movement• Increased tone (not necessarily constant)• Pathological reflexes (increased reflexes: hyperreflexia and/or pyramidal signs e.g. Babinski response). Spastic bilateral CP: Limbs of both sides of the body are involved. Spastic unilateral CP: Limbs on one side of the body are involved.
Dyskinetic type: Dyskinetic CP is dominated by both: <ul style="list-style-type: none">• Abnormal pattern of posture and/or movement• Involuntary, uncontrolled, recurring movement Dyskinetic CP may be either dystonic CP or chorea-athetotic CP: Dystonic CP is dominated by both: <ul style="list-style-type: none">Hypokinesia (reduced activity)Hypertonia (tone usually increased) Chorea-athetotic CP is dominated by both: <ul style="list-style-type: none">Hyperkinesia (increased activity)Hypotonia (decreased tone)
Ataxic type: Ataxic type is characterized by both: <ul style="list-style-type: none">• Abnormal pattern of posture and/or movement• Loss of muscular coordination so that movements are performed with abnormal force, rhythm and accuracy.

In general, neurological abnormalities identified as the spastic present during sleep and do not change with activity or emotional stress. A child with spastic cerebral palsy is typically prone to developing earlier contractures and having more frequent problems than does a child with dyskinetic CP⁽¹⁴⁾. In the dyskinetic form, the movements typically begin after the second year of life and progress slowly for several years, persisting into adulthood⁽¹⁴⁾. They involve the upper extremities more frequently than the lower extremities⁽¹⁴⁾. Oral-motor dysfunction and tongue thrusting are common symptoms⁽¹⁴⁾. These movements show marked variability depending on the state of the individual; they are decreased during relaxation and sleep and increased during anxiety and stress⁽¹⁴⁾. Dyskinetic forms tend to occur typically in term infants with perinatal asphyxia or kernicterus⁽¹⁴⁾. Children with a combination of spastic and dyskinetic types are labelled as having a mixed type⁽¹⁴⁾.

Children with the ataxic type usually due to damage of the cerebellum in prenatal time ⁽⁸⁸⁾(e.g., fetal alcohol syndrome).

1.1.4.2 Severity of Cerebral Palsy According to Gross Motor Function Classification System (GMFCS):

The most commonly used classification of gross motor function in children with CP is the **G**ross **M**otor **F**unction **C**lassification **S**ystem (GMFCS). This system a very simple and well-recognized classification of mobility in CP, was introduced by Palisano and Rosenbaum in 1997^(27, 33, 34, 35). According to the system, function is divided into five levels; children in Level I have the most independent motor function and children in Level V have the least⁽²⁶⁾. Distinction between the levels is thought to be clinically meaningful and is based on functional abilities and limitation (i.e., self-initiated movement, sitting, transfers and need for hand-held mobility devices such as walkers or wheeled mobility)^(14, 26, 33, 34, 35)(Tab.3). Each level of the GMFCS provides functional descriptions for five age bands: before 2, 2 to 4, 4 to 6, 6 to 12 and 12 to 18 years.

Tab. 3. Gross Motor Function Classification System (GMFCS) Levels 1-5 at age 6-12 years ⁽³⁶⁾ .	
 <p>GMFCS Level I</p>	<p>GMFCS Level I:</p> <p>Children walk indoors and outdoors and climb stairs without limitation. Children perform gross motor skills, including, running and jumping; but speed, balance and coordination are impaired.</p>
 <p>GMFCS Level II</p>	<p>GMFCS Level II:</p> <p>Children walk indoors and outdoors and climb stairs holding onto a railing but experience limitations walking on uneven surfaces, in crowds and for long distances.</p>
 <p>GMFCS Level III</p>	<p>GMFCS Level III:</p> <p>Children walk indoors or outdoors on a level surface with an assistance mobility device and may climb stairs holding onto a railing. Children may use wheelchair mobility when traveling for a long distance.</p>
 <p>GMFCS Level IV</p>	<p>GMFCS Level IV:</p> <p>Children use methods of mobility that usually require adult assistance. They may continue to walk for short distances with physical assistance at home but rely more on wheeled mobility outdoors.</p>
 <p>GMFCS Level V</p>	<p>GMFCS Level V:</p> <p>All areas of motor function are limited. Children have no means of independent mobility and are transported by an adult. There is an inability to maintain anti-gravity head and trunk posture.</p>

The following curves (FIG.1) are useful for monitoring the development of motor function in children with CP and predicting future outcomes. They are useful for identification a child's developmental status at a specific point in time in relation to the age and gross motor function. If the GMFCS-level is known, the prediction of a young person's expected function can be made with some confidence ⁽¹⁴⁾.

The vertical lines on the gross motor curves indicate the point at which 90% of final gross motor is likely to be achieved. The GMFCS becomes more reliable in older age groups starting at 6-12 age band⁽²⁷⁾. A child who is between 2 and 4 years old may be on the upswing of their gross motor curve, a child who is 6-12 years old may be on a stable plateau of gross motor function, and a youth between 12 and 18 years may be on a descending curve of gross function⁽²⁷⁾.

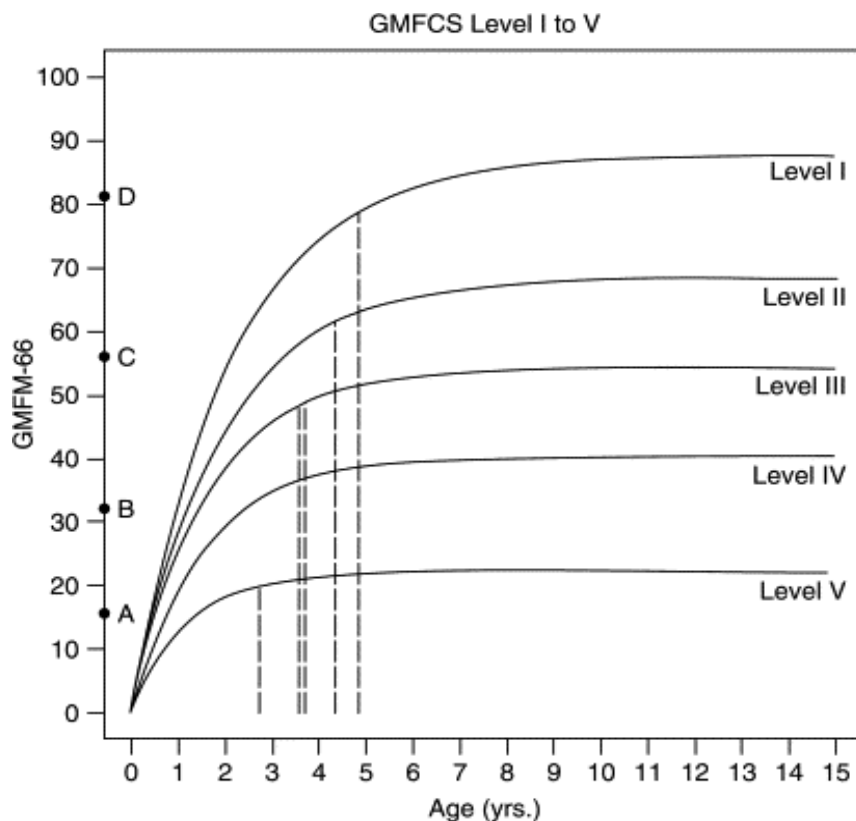


FIG. 1. Gross motor curves. The curves provide information about the predicted average development in groups designated by the GMFCS⁽²¹⁾.

1.2 Periventricular Leukomalacia (PVL):

1.2.1 Definition of Periventricular Leukomalacia:

Periventricular Leukomalacia (PVL) is caused by a hypoxic-ischemic damage to white matter in premature infants⁽²⁸⁾. PVL is the most important factor of CNS morbidity in very low birth weight infants (<1500 grams) and occurs mainly between 26-34 weeks of gestational age before myelination of oligodendrocytes and myelin basic protein⁽³²⁾. PVL is occasionally reported to occur in full-term infants.

1.2.2 Pathology of Periventricular Leukomalacia:

Periventricular leukomalacia is a primary arterial ischemic injury to white matter.

It is expected that the predisposing factors are as follows^(31, 29):

1. Vascular immaturity in the deep WM
2. Vulnerability of differentiation glia, particularly pre-oligodendrocytes, to glutamate and cytokines

During hypotensive episodes, hypoxic-ischemic insults in the arterial end-zones may cause a lesion of immature white matter⁽²⁷⁾. The pathology of this lesion is necrosis of all cell types and axonal pathways coursing adjacent to the ventricles with or without cyst formation⁽²⁷⁾. Microscopically, there is axonal and cellular coagulative necrosis, which is separated from the ventricles by glial tissue produced by the reformed cytoplasm of the reactive astrocyte, microglial activation, foam cell infiltration, reactive astrogliosis and neovasculation.

A perifocal edema may present as softening of the adjacent tissue⁽³¹⁾.

The lesions of PVL are classically bilateral, measure 2-6 mm in diameter, and are within 15 mm of the ventricular wall⁽³⁰⁾. The most common locations are anterior to the frontal horn (FIG 2, 3), angles of the lateral ventricles at the level of the foramen of Monro, and lateral regions of the trigone and occipital horn, including the optic radiation⁽³⁰⁾. The relationship of these widespread lesions in the periventricular region, is unclear. In the extreme cases, necrotic foci extend from the periventricular sites for a variable distance into the centrum semiovale, rarely as far as the subcortical white matter⁽³⁰⁾. In the chronic stage, the entire white matter may have undergone multiple cavity formations, in contrast to preserved cerebral cortex and deep grey nuclei⁽³⁰⁾. In the course of absorption, the lesion becomes cystic cavitation clustering around the lateral ventricles which contain cell debris (FIG.4, 5, 6) and finally a ventricular enlargement is seen^(29, 31). This leads to a reduction in the volume of the brain with enlargement of the lateral ventricles and a thin corpus callosum.



FIG. 2. Periventricular leukomalacia (PVL), note the multiple white spots (necrotic foci) in periventricular white matter⁽²⁹⁾.

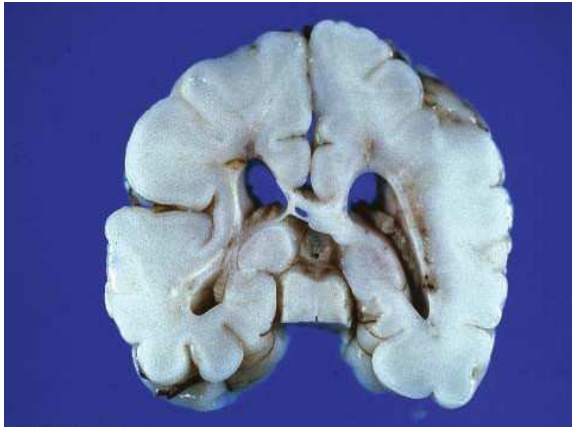


FIG. 3. Macroscopic appearance of the PVL lesions. There are white opaque lesions in the periventricular white matter in this brain 29 days after birth⁽²⁹⁾.



FIG. 4. Periventricular leukomalacia. Note the dilated ventricles and reduced white matter volume⁽²⁹⁾.

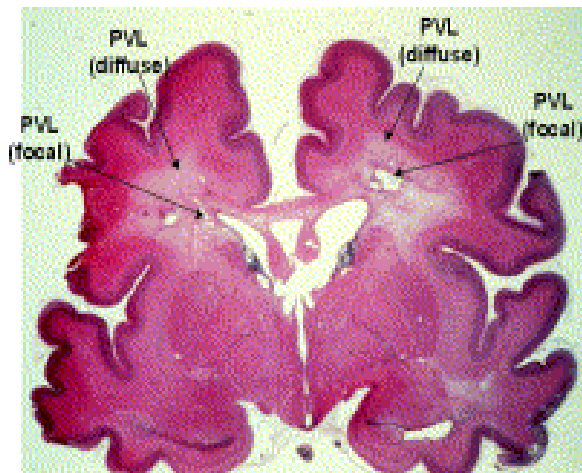


FIG. 5. PVL Coronal section of the cerebrum.

Note the two components of the lesion, deep focal areas of cystic necrosis and more diffuse cerebral white matter injury⁽²⁹⁾.

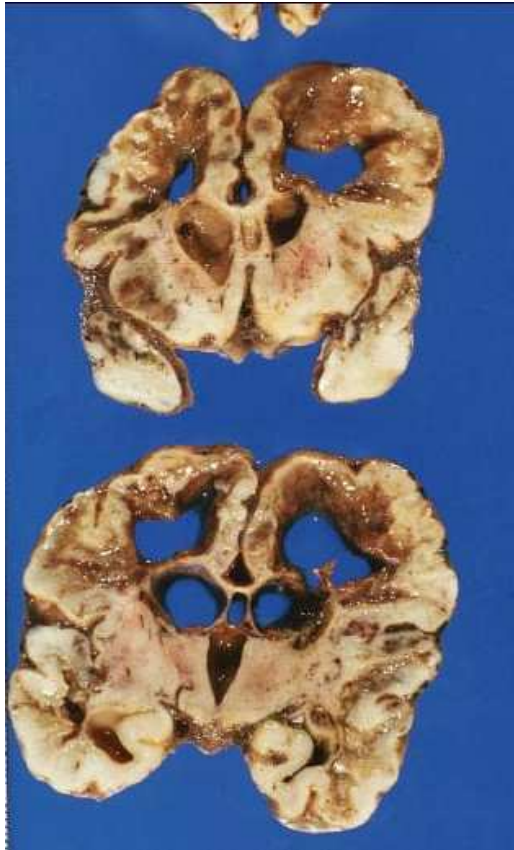


FIG. 6. Multicystic leukomalacia present in the brain of a neonate at the time of death (three days of age). There is marked destruction of the white matter⁽²⁹⁾.

1.2.3 Pathophysiology of Periventricular Leukomalacia:

We know that in PVL, the necrosis of white matter occurs mostly near the lateral ventricles, where the corticospinal tract runs. The corticospinal tract, which carries the motor information from the brain to the rest of the body, originates from pyramidal cells in layer V of the cerebral primary motor cortex. It consists of axons of the upper motor pathway which extend downward from the upper motor neurons and from the corona radiata. These axons descend passing through the posterior limb of the internal capsule and transverse dorsal and lateral the external angle of the lateral ventricle and run then through the midbrain, where the fibers concerned to the upper body are situated medially while those concerned to the lower body are placed laterally. They travel down through the cerebral peduncle and then spinal cord⁽⁴⁵⁾. The injury to these axons produces the typical clinical picture of spastic cerebral palsy, in which the most prominent motor impairment is in the legs⁽²⁷⁾(FIG.7).

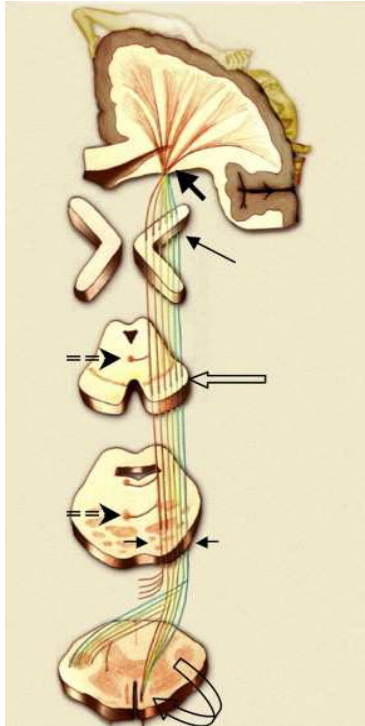


FIG. 7. shows the motor tract. Dark thick arrow shows the motor tract originates from motor cortex. Thin black arrow shows motor tract descending through the internal capsule. White arrow shows motor tract descending through cerebral peduncle and then through pons and finally through spinal cord⁽⁸¹⁾.

1.3 The Role of Imaging in PVL:

1.3.1 The Role of Ultrasound in PVL:

In the acute phase of PVL, the early sonographic sign of periventricular white matter injury is the periventricular flare; an area shows loss of normal parenchymal echoes. The more severely damaged tissue shows edema as an echogenic zone. The timing of cavitation varies but typically appears on ultrasound 2 to 4 weeks after injury⁽³⁸⁾ (FIG. 8).

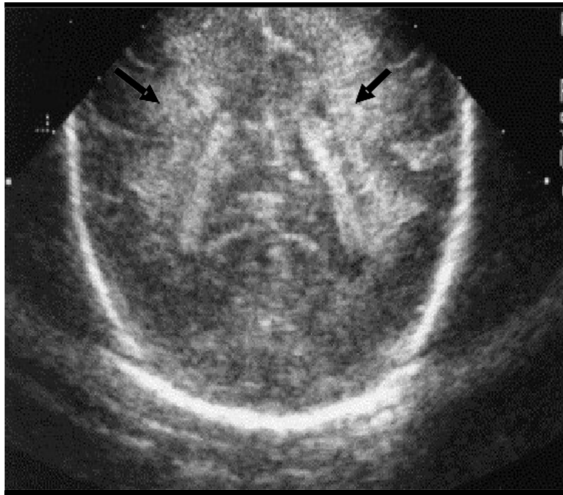


FIG. 8. (a) Coronal ultrasound view from preterm infant at 5 days of age. Note the increase echogenicity within periventricular white matter⁽⁴⁶⁾.

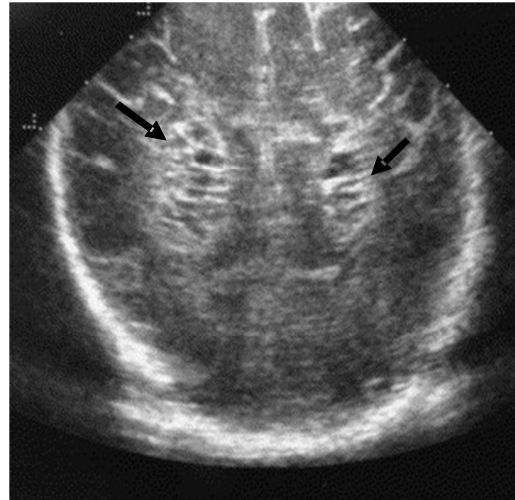
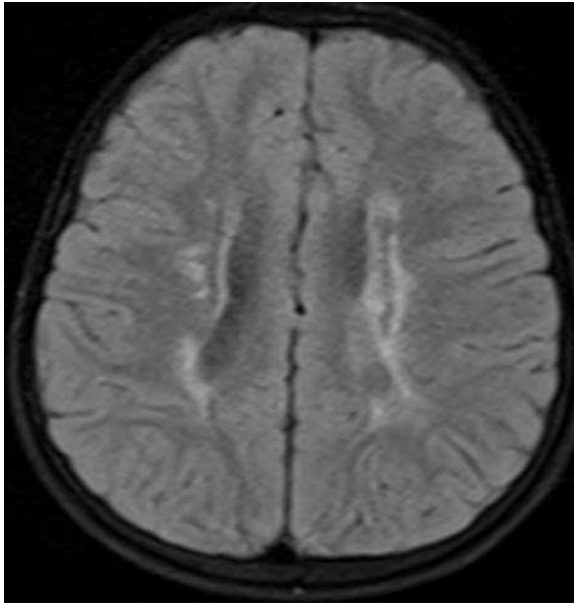


FIG. 8. (b) Coronal ultrasound from the same infants 2 weeks later. Note the evolution to diffuse cyst formation⁽⁴⁶⁾.

1.3.2 The Role of MRI in PVL:

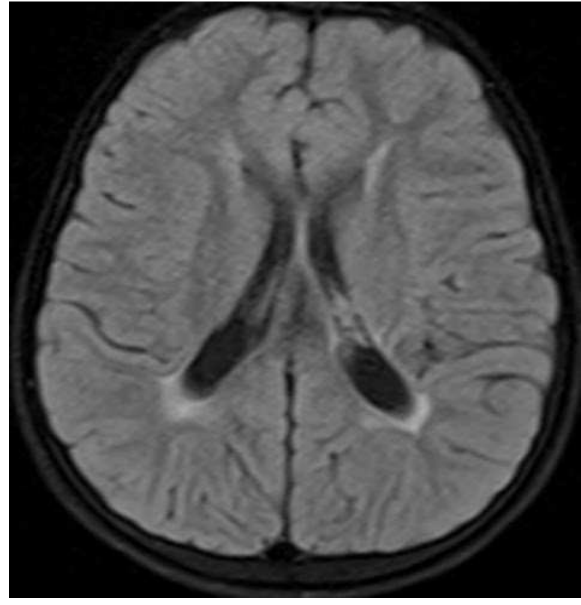
MR imaging techniques have been used as the gold standard in documenting periventricular white matter lesions⁽⁷³⁾. The typical MR imaging findings by PVL are (28, 38):

- 1- increased signal intensity, i.e., gliosis in the periventricular white matter on T2-weighted and on Flair (FIG.9.(a)). Similar changes (increased signal intensity) can occur due to metabolic and inflammatory changes, for example, the leukodystrophy. In leukodystrophy, the lateral ventricle is curved and not cornered extracted. In PVL, the gliosis is adjacent to the posterior horn and the lateral ventricles and leads to cornered edged attraction of the lateral ventricles (FIG.9. (b)).
- 2- ventricular enlargement with an irregular outline of the body and trigone of the lateral ventricles (FIG.9(c)).
- 3- thinning of the corpus callosum, most commonly the posterior body, splenium, and isthmus (FIG.9(d)).
- 4- abnormally and delayed myelination.
- 5- reduced quantity of white matter, always at the trigone but in severe cases involving the whole centrum ovale.



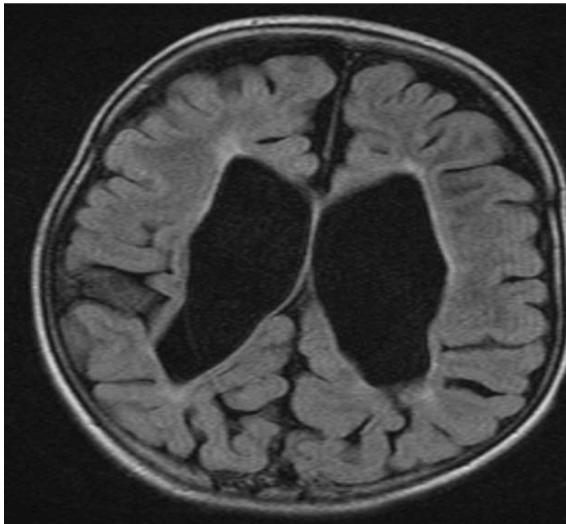
a

FIG. 9. (a) MRI axial flair, five years old-child with bilateral spastic cerebral palsy, note the increased signal intensity in the periventricular white matter.



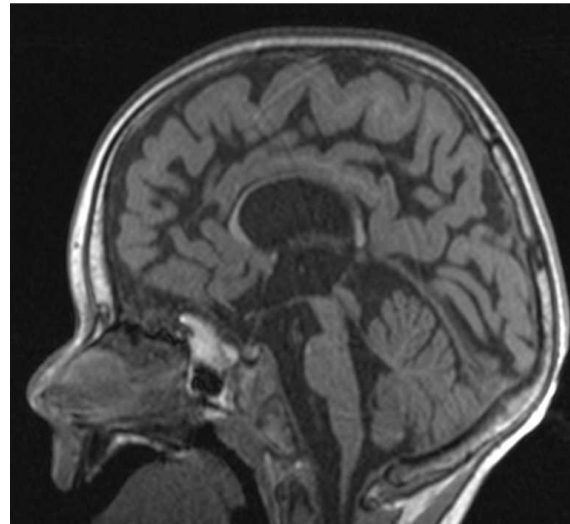
b

FIG. 9. (b) MRI axial flair, the same patient, the lateral ventricles are extended and atypical configured.



c

FIG. 9. (c) MRI flair axial, 18 months-old infants with CP, GMFCS grade IV. Note the ventricular enlargement with an irregular outline of the lateral ventricles.



d

FIG. 9. (d) MRI sagittal T1-weighted, note the thinning of the corpus callosum and the reduced quantity of white matter.

1.4 Previous Clinical Studies:

E. Melhem et al. (2000) established that the severity of the motor impairment in children with PVL correlates with the mean lateral ventricular volumes which could be used as an indirect predictor of motor and cognitive outcome in children with spastic CP and PVL. The patients in this study were classified according to the motor deficit into three groups: mild, moderate and marked motor impairment⁽³⁹⁾.

Another study G. Serdaroglu et al. (2004) showed that the PVL grades III and IV, gliosis numbers over three, thinning of the corpus callosum and presence of cortical atrophy were risk factors for developmental delay in patients with cerebral palsy. The patients in this study were classified according to the motor deficit into four groups: normal, mild, moderate and marked motor impairment⁽⁴⁰⁾.

A third study in USA, A. Panigrahy et al. (2005) showed a positive correlation between the thickness of the mid-body of the corpus callosum and the volume of cerebral white matter in children with cerebral palsy, which was significantly less in the spastic cerebral palsy group than in the two other groups of children (groups of hypotonia and group of no specific neuromotor abnormality). A correlation with the severity of CP was not carried out, and all children with CP were grouped together⁽⁴¹⁾.

G. Cioni et al. (1999) have studied the correlation between visual function and neurodevelopmental outcome in children with PVL. The visual impairment was the most important variable in determining the neurodevelopmental scores of these infants, more than their motor disability and the extent of their lesions on MRI⁽⁴²⁾. In this study, the correlation between MRI-findings and motor disability was not carried out.

A study from S. Fukuda et al. (2010) showed that the volume of thalami is reduced in infants with PVL compared with the other group infants. A correlation between the severity of CP and the volume of thalami was also not carried out⁽⁴³⁾.

A study from Panigrahy (2001) did not show any correlation between the gliosis and the clinical neuromotor abnormality⁽⁴¹⁾. A study from Fedrizzi (1996) shows lacks of correlation between T2 prolongation in the affected periventricular white matter and the severity of neuropsychologic deficit⁽⁷⁴⁾ too.

2 Aim of the Study:

Until now, existing studies in patients with PVL and cerebral palsy could not clarify the relationship between the severity of damage in the cerebral MRI and the severity of motor deficit, as it is now based on GMFCS levels. If we find a correlation between a surrogate parameter and the gross motor function level, we can predict the future of the motor performance of the patient far before the completion of the 2nd year of life, that would be useful for facilitating the dialogue between doctors, therapists and parents and for planning of intensive motor in the early years of motor development. The aim of this study was to answer the following questions:

- is there any correlation between GMFCS level and the MRI-findings?
1. corpus callosum: length of corpus callosum, thickness of genu, thickness and location of the thinnest part of corpus callosum
 2. brainstem (diameter of midbrain, cerebral peduncles and pons)
 3. lateral ventricles
 4. gliosis
 5. existence of small porencephalic cysts
 6. existence of microhemorrhages
- Which MRI-parameter correlates most likely with GMFCS level?

3 Methods:

3.1 Study Design:

This is a retrospective data analysis of existing patient's data. The MRI examinations were exclusively performed in the Institute of Clinical Radiology Campus Grosshadern (Director of the Institute: Prof. Dr. med. M. Reiser) under the medical supervision of Prof. Dr. med. B. Ertl-Wagner (neuroradiologist). The clinical data was assessed at the Department of Pediatric Neurology at Dr. Von Hauner Children's Hospital, University of Munich (Director: Prof. Dr. med. Dr. sci. nat. C. Klein), under the supervision of Prof. Dr. med. F. Heinen and at the kbo Children's Centre in Munich, (Prof. Dr. med. V. Mall). The study was performed with permission of the local ethics committee (Ethikkommission der LMU München, Projekt-Nr: 500-11).

3.2 Subjects:

All patients with periventricular white matter hyperintensities on cranial MRI-examination from October 2003 to April 2011 were reviewed for the following clinical data (Tab.4).

Tab. 4. Clinical Data of the patients in our study.	
Identification number	
Date of birth	
Gestational age at birth (weeks)	
Date of MRI/corrected age at the date of MRI-examination	
Type of CP: bilateral/unilateral spastic CP/mixed type	
Severity of CP according to GMFCS (I-V)	
Existence of hemorrhage, hydrocephalus, shunt, porencephaly or brain malformation	
Existence of other diseases, e.g. congenital infection.	

In order to improve patient's data quality; we have excluded all patients with:

- ✗ Clinical picture of unilateral cerebral palsy
- ✗ Patients less than 12 months of age at the date of MRI examination. Because it is not possible to distinguish the premyelinated periventricular white matter hyperintensity from abnormal periventricular white matter hyperintensity
- ✗ Patients with perinatal brain damage other than PVL (e.g. hemorrhage, porencephaly, hydrocephalus with or without VP-Shunt) and patients with brain malformation (e.g. Septo-optic dysplasia)
- ✗ Patients with periventricular hyperintensity related to other diseases (e.g. congenital CMV infection)

To know if the severity of prematurity may influence the severity of CP, we have divided the patients according to gestational age at delivery into 4 subgroups: extremely preterm (<28 weeks), very preterm (28 to <32 weeks), moderate to late preterm (32 to < 37 weeks) and term infants \geq 37 weeks⁽⁸⁹⁾(Tab.5).

Tab.5. Groups of patients according to gestational age at delivery.			
Extremely preterm	Very preterm	Moderate to late preterm	Term infants
<28 weeks	28 to < 32 weeks	(32 to < 37 weeks)	\geq 37 weeks

3.3 MRI-Protocol:

All patients who met the clinical and MR imaging criteria and underwent a standard pediatric brain MRI: axial flair, axial and sagittal T2-weighted and axial T1-weighted, were included in our study.

Tab. 6. MRI-parameters; which were measured in our study.	
Study of the corpus callosum	Midsagittal T2-weighted image
	anterior-posterior diameter of the skull in cm
	length of the corpus callosum (FIG.10) in cm
	thickness of the genu (FIG.10) in mm
	location of the thinnest point of corpus callosum (FIG.17)
Study of the brainstem	thickness of the corpus callosum at its thinnest point (FIG.10) in mm
	Midsagittal T2-weighted image
	craniocaudal diameter of the pons (FIG.10) in mm
	transverse diameter of the midbrain (FIG.10) in mm
	Axial T1-weighted image
Study of the lateral ventricle	axial diameter of the midbrain (FIG.11) in mm
	axial diameter of the cerebral peduncles (FIG.11) on both sides in mm
	Axial T2-weighted image
	grade of extension of the lateral ventricle (I-V) (FIG.12)
	width of the posterior horn of the lateral ventricle at its widest point (FIG.13 a) on both sides in mm
Study of the gliosis	distance between lateral ventricles and cortex (FIG.13 b) on both sides in mm
	distance between lateral-extraction of lateral ventricles and cortex (FIG.13 b) on both sides in mm
	depth of lateral extraction of lateral ventricles (FIG.13 c) on both sides in mm
	Axial flair image
	gliosis grade I-V grade (FIG.14)
Study of porencephalic cyst	width of the gliosis (FIG.15 a) on both sides in mm
	distance between the gliosis and the cortex (FIG.15 b) on both sides in mm
Study of microhemorrhages	existence of small porencephalic cysts "black holes" on axial flair: yes/ no (FIG.16 a)
	existence of microhemorrhages on T2*-Weighted gradient echo sequence (yes/ no) (FIG.16b)

The MRI parameters were manually measured from the cerebral MRI by the same board certified neuroradiologist who was unaware of the clinical findings (Tab. 6). The neuroradiologist has measured the length of the corpus callosum from the anteriormost aspect of the genu to the posteriormost aspect of the splenium and the thickness of the genu (FIG.10). Similar to Witelson's scheme; the corpus callosum was divided into 7 subregions: 1, rostrum; 2, genu; 3, rostral body; 4, anterior midbody; 5, posterior midbody; 6, isthmus; 7, splenium (FIG.17). According to the above scheme, she has determined the location of the thinnest point of corpus callosum and measured it.

The transverse diameter of the midbrain and the craniocaudal diameter of the pons were measured by using midline sagittal T2-weighted images (FIG.10). The axial diameters of midbrain and cerebral peduncles were measured by using axial T1-weighted image (FIG.11).

By using axial images T2-weighted distance between lateral ventricles and cortex (FIG.13 a), distance between lateral-extraction of lateral ventricles and cortex (FIG.13 b) and the depth of lateral extraction of lateral ventricles (FIG.13 c) were measured. Right and left hemispheric involvement were measured separately and merged.

By using axial flair image; the neuroradiologist has measured the width of the gliosis and the distance between the gliosis and the cortex.

By using axial flair, she has determined the existence of small porencephalic cysts and by using T2*-Weighted gradient echo sequence, she has determined the existence of microhemorrhages. She has rated the quality of the investigation (i.e. existence of artefacts) and the existence of other norm variation (e.g. arachnoid cyst) or malformation (Dandy-Walker syndrome).

As in our study the participant age at the time of MRI ranged from 12 to 212 months, the greatest anterior-posterior diameter of the skull from the inner table of the frontal bone to the inner table of the occipital bone was measured. Similar to Barkovich⁽⁹¹⁾ the ratios of the length of the corpus callosum, transverse diameter of midbrain, diameter of the pons and width of lateral ventricles were determined by dividing them by the anteroposterior (AP) diameter of the skull. As the ratios of thickness of genu, diameter of pons, diameters of midbrain to AP diameter of the skull were too small, we have these ratios 10 times doubled.

The neuroradiologist have classified the width of the LV (FIG.12) and the width of the gliosis according to the optic view into 5 grades with grade 1 the least and grade 5 the most grade (FIG.14). She has rated the quality of the investigation (i.e.

existence of artefacts) and the existence of other norm variation (e.g. arachnoid cyst) or malformation (Dandy-Walker syndrome).

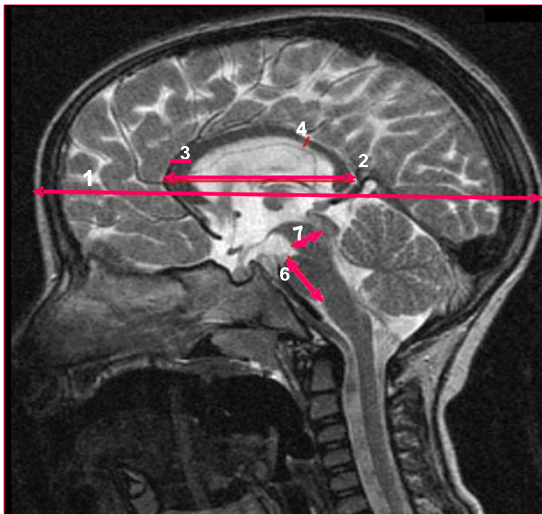


FIG. 10. Midsagittal T2-weighted image. MRI-parameters:

anterior-posterior diameter of the skull (arrow number 1), length of corpus callosum (arrow number 2), thickness of the genu of the corpus callosum (arrow number 3), thickness of the corpus callosum at its thinnest point (arrow number 4), craniocaudal diameter of the pons (arrow number 6), transverse diameter of the midbrain (arrow number 7).

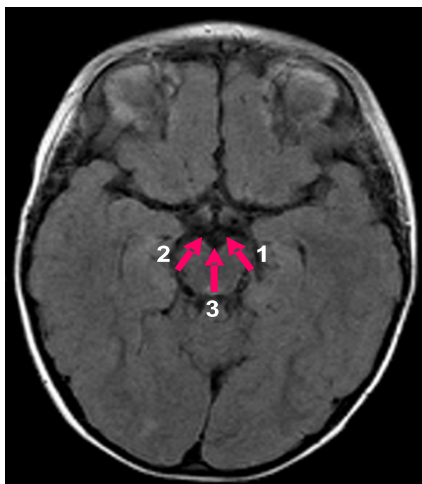


FIG. 11. Axial T1-weighted images. Axial diameter of the cerebral peduncles (left arrow number 1) and right (arrow number 2). Axial diameter of the midbrain (arrow number 3).

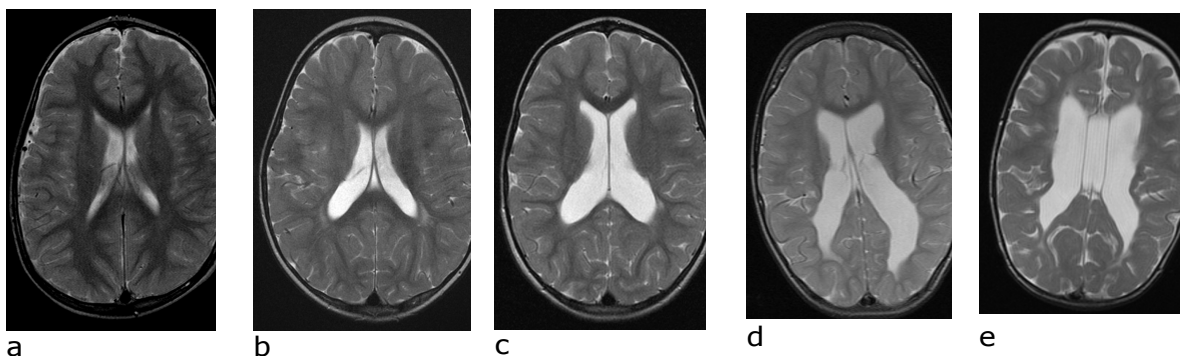


FIG. 12. Axial T2-weighted MR images: show the optic classification of the extension of the lateral ventricle according to the width with grade 1 the least and grade 5 the most grade. a: grade 1, b: grade 2, c: grade 3, d: grade 4, e: grade 5.

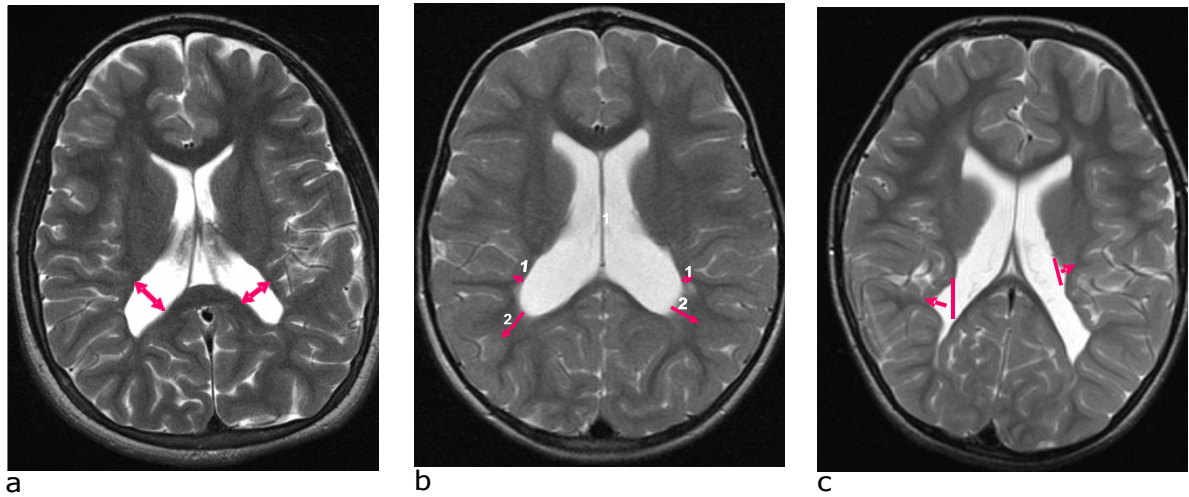


FIG. 13. Axial T2-weighted MR images show: a: width of the posterior horn of the lateral ventricle (right, left) at its widest point, b: distance between the lateral ventricles and the cortex (right, left) (arrow number 1), distance between the lateral expansion of the ventricles and the cortex (right, left) (arrow number 2). c: depth of lateral expansion of lateral ventricles.

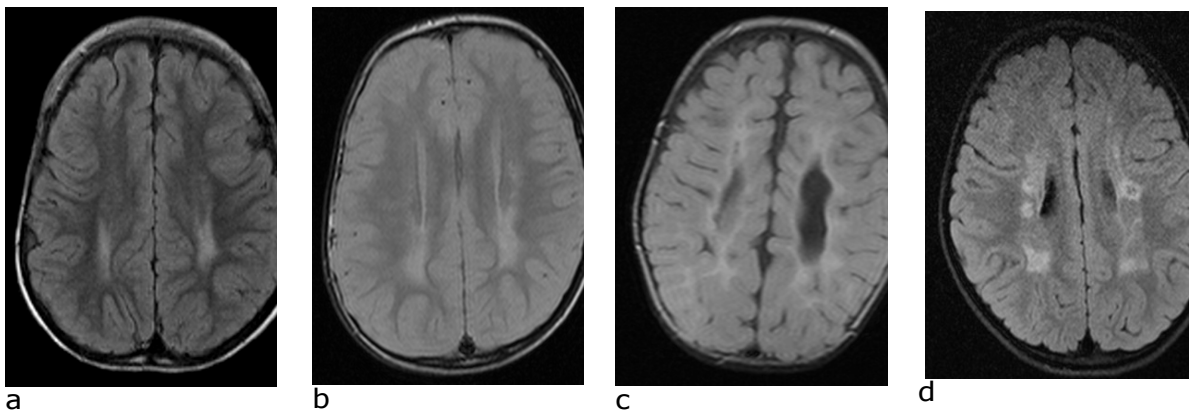


FIG. 14. Axial FLAIR MRI: optic classification of the grade of the gliosis: a, gliosis grade 2; b, gliosis grade 3; c, gliosis grade 4; d, gliosis grade 5.

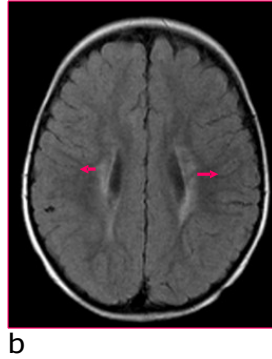
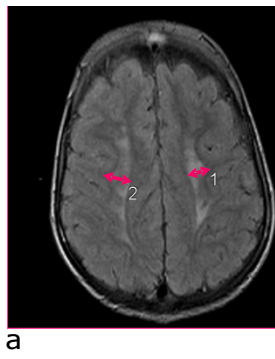


FIG. 15. Axial flair MRI. a, Width of the gliosis on the right and on the left; b, distance between the gliosis and the cortex on the right and on the left.

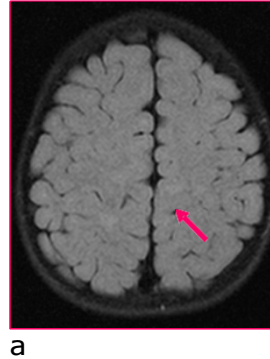


FIG. 16. a, axial flair shows a small porencephalic cyst. b, axial T2*-weighted gradient echo sequence shows the deposits of microhemorrhages in a patient with PVL.

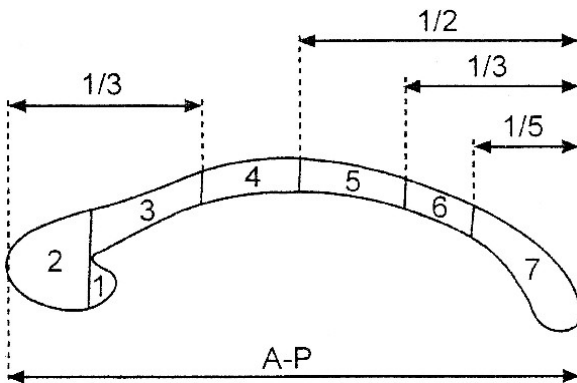


FIG. 17. Witelson's scheme^(44, 61). Corpus callosum subregions: 1, rostrum; 2, genu; 3, rostral body; 4, anterior midbody; 5, posterior midbody; 6, isthmus; 7, splenium; AP: length of anterior-posterior line.

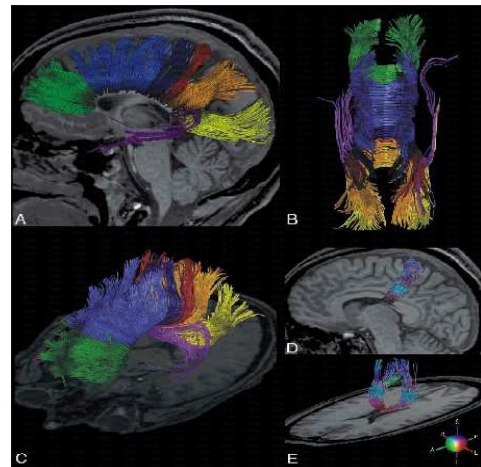


FIG. 18. Transcallosal fiber tracts from a single male subject overlaid onto individual anatomical reference images. Reconstruction of all callosal fibers comprising bundles projecting into the prefrontal lobe (coded in green), premotor and supplementary motor areas (light blue), primary motor cortex (dark blue), primary sensory cortex (red), parietal lobe (orange), occipital lobe (yellow), and temporal lobe (violet). (D and E) sagittal and oblique views of callosal fiber tracts that project into the primary motor cortex⁽⁶¹⁾.

3.4 Statistical Analysis:

Statistical analysis was performed using SPSS Program (IBM SPSS Statistic Version 20, Illinois, USA). Using the descriptive statistic, we have measured the distribution of the patients according to gestational age and according to the severity of cerebral palsy using circle graph. We have used the Pearson rank Correlation to measure the correlation between the following variables (Tab.7). A p -value of less than 0,05 was taken as significant⁽⁴⁸⁾.

Tab. 7. Correlation between the following variables	
Severity of CP	Gestational age
	Corrected age at the time of MRI
	MRI-findings
Correlation between right and left of MRI-findings	
Gestational age	MRI-findings

We have measured the mean value, median, standard deviation and 95% confidence interval of the above parameters at the different levels of GMFCS using box plot, linear, scatter plot and error bar diagrams.

Tab. 8. Interpretation of Correlation Coefficient ⁽⁴⁸⁾	
Correlation coefficient Value	Strength of the correlation
-1,0	Perfectly negative
-0,8	Strongly negative
-0,5	Moderately negative
-0,2	Weakly negative
0,0	No association
+0,2	Weakly positive
+0,5	Moderately positive
+0,8	Strongly positive
+1,0	Perfectly positive

4 Results:

4.1 Total Cohort Characteristics:

Out of 89 screened patients, we have found 50 children (27 males, 23 females) between the age of 12 months and 17 years fulfilled the criteria of bilateral spastic cerebral palsy and MRI finding of PVL (FIG.19).

Tab. 9. The descriptive statistic of patients in our study				
Variable	Minimal	Maximal	Mean	SD
Gestational age at time of birth (weeks)	26	39	31,80	3,08
Age at time of MRI (months)	12	212	69,66	60,17
Anterior-Posterior diameter of Skull (cm)	15	22	17,02	1,43
Axial diameter of the midbrain (mm)	9	17	12,72	1,85
Axial diameter of cerebral peduncles on the left (mm)	9	17	12,11	1,8
Axial diameter of cerebral peduncles on the right (mm)	10	16	12,02	1,56
Craniocaudal diameter of pons (mm)	12	27	21,24	3,05
Sagittal diameter of midbrain (mm)	8	15	10,47	1,38
Grade of gliosis 1 to 5	2	5	3,10	1,04
Width of gliosis on the left (mm)	2	16	8,17	3,57
Width of gliosis on the right (mm)	2	18	8,39	3,91
Grade of extension of LV 1 to 5	1	5	2,18	1,16
Width of posterior horn of LV on the left (mm)	4	25	11,67	4,49
Width of posterior horn of LV on the right (mm)	4	22	10,48	3,7
Depth of extraction of LV on the left (mm)	0	5,0	1,86	1,26
Depth of extraction of LV on the right (mm)	0	4,5	1,51	1,23
Distance between extraction of LV and Cortex on the left (mm)	0	15,0	4,35	3,49
Distance between extraction of LV and Cortex on the right (mm)	0	11,0	4,17	3,26
Distance between LV- Cortex on the left (mm)	0	6,5	1,81	1,52
Distance between LV- Cortex on the right (mm)	0	6,5	1,69	1,51
Distance between gliosis and Cortex on the left (mm)	0	18,0	1,69	2,68
Distance between gliosis and Cortex on the right (mm)	0	5,0	1,36	1,27
Length of CC (cm)	4	7	5,71	0,76
Thickness of the thinnest part of CC (mm)	0,5	4,5	1,89	0,88
Thickness of genu (mm)	1	13	7,69	2,64
Existence of small porencephalic cyst	0	1	,34	0,48
Existence of microhemorrhage in	0	1	0,06	0,25
Artifact1to 5	1	4	1,28	0,76

Tab. 10. Correlation between the following variables and gestational age and GMFCS according to Pearson's rank correlation			Gestational age		GMFCS Level	
			r Value	p Value	r Value	p Value
Date of MRI			-0,078	0,59	-0,14	0,29
GMFCS			-0,23	0,11		
Brainstem	Axial diameter of midbrain/anterior-posterior diameter of the skull X 10		0,21	0,15	-0,21	0,14
	Sagittal diameter of midbrain/anterior-posterior diameter of the skull X 10		0,27	0,11	-0,48	<0,001
	Sagittal craniocaudal diameter of pons/anterior-posterior diameter of the skull X 10		0,1	0,48	-0,2	0,17
	Diameter of cerebral peduncle/anterior-posterior diameter of the skull		0,2	0,18	-0,41	<0,05
Measurement of corpus callosum	Length of CC/anterior-posterior diameter of the skull		-0,14	0,34	-0,43	<0,001
	Thickness of genu/ anterior-posterior diameter of the skull X 10		-0,12	0,4	-0,5	<0,001
	Thickness of the thinnest part of CC		-0,12	0,41	-0,48	<0,001
Measurement of gliosis	Grade of gliosis		-0,16	0,28	0,27	0,06
	Width of gliosis on both sides		0,29	<0,05	0,15	0,29
	Distances between gliosis on both sides and cortex		-0,19	0,19	-0,46	<0,001
Measurement of Lateral ventricle	Grade of LV- extension		0,14	0,32	0,5	<0,001
	Distances between LV on both sides and cortex		0,01	0,96	-0,54	<0,001
	Distances between extraction of LV on both sides and cortex		-0,13	0,4	-0,04	0,77
	Width of posterior horn on both sides/anterior-posterior diameter of the skull		-0,14	0,32	0,44	<0,001
	Depth of extraction of LV on both sides		-0,2	0,17	0,57	<0,001
Existence of small porencephalic cyst			0,1	0,48	0,2	0,17
Existence of microhemorrhage			-0,16	0,44	0,27	0,17

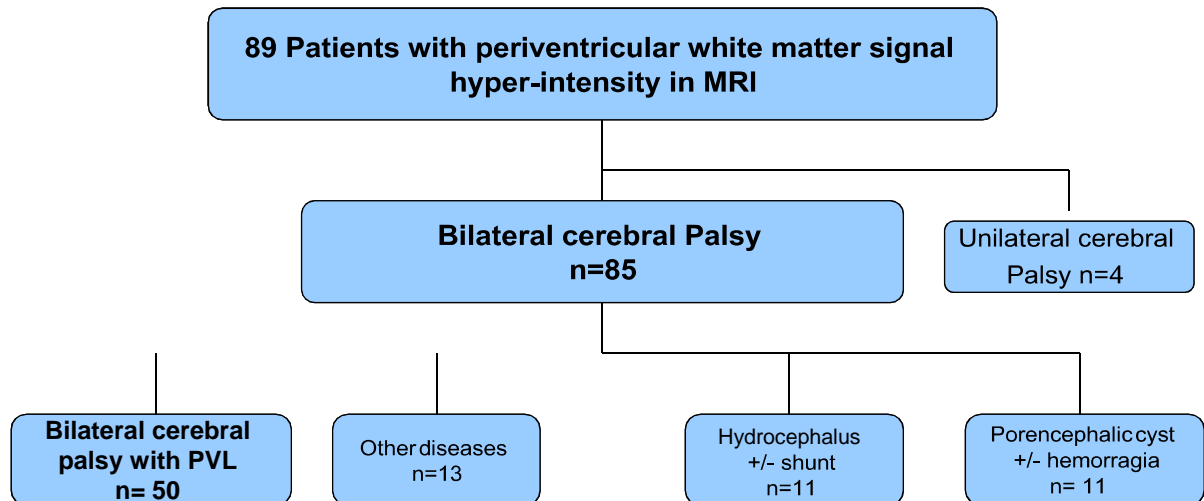


FIG. 19. Flow diagram for determination of patients' collective.
Other diseases (e.g. brain malformation, connatal infections).

4.2 Subgroups Data of Patients according to GMFCS Level:

42 children (84%) have spastic cerebral palsy, and 8 children (16%) have mixed type (spastic and dyskinetic cerebral palsy).

The most common levels of cerebral palsy according to GMFCS in our study were level I and II (26%), followed by level III (22%) then level IV (20%). The least common level of cerebral palsy was level V (6%).

We did not find a significant correlation between the severity of BS-CP and the type of CP (spastic/mixed). However, at level IV of cerebral palsy 30% of the patients have mixed type of cerebral palsy and at level V 33%.

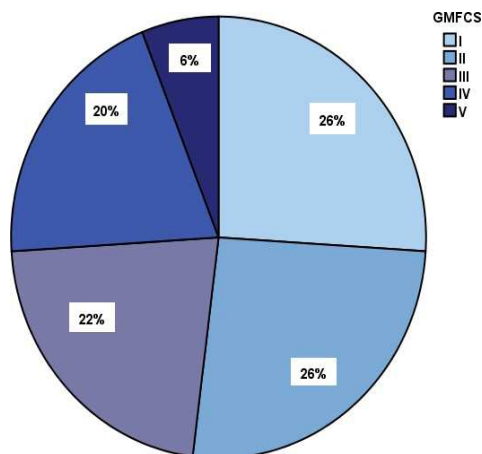


FIG. 20. Distribution of patients according to GMFCS

Tab. 11. Distribution of patients according to type of CP by GMFCS						
	totals	GMFCS I	GMFCS II	GMFCS III	GMFCS IV	GMFCS V
N	50	13	13	11	10	3
Mixed Type	8	1	1	2	3	1
Percent	16%	8%	8%	18%	30%	33%
r and p	$r = 0,25$ $p = 0,78$					

4.2.1 Correlation between GMFCS Level and gestational Age at Birth:

The gestational age at birth (mean 31,80 — 3,08 weeks) ranged from 26-39 weeks. The severity of BS-CP according to GMFCS located by term infants between level I and III (FIG 22). The severity V was only found in preterm infants, who were born between 28 to <32 weeks.

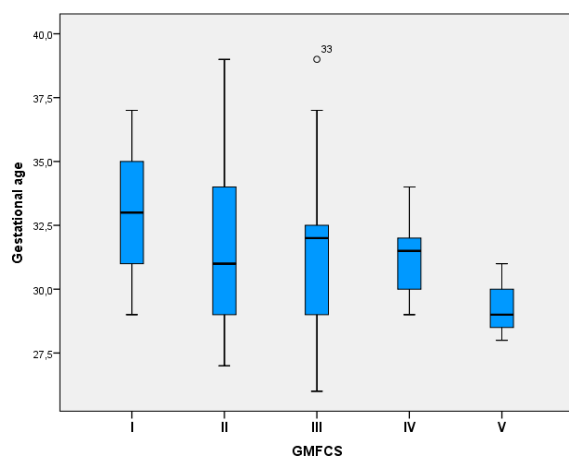


FIG. 21. Box plot of patients according to GMFCS by gestational age.

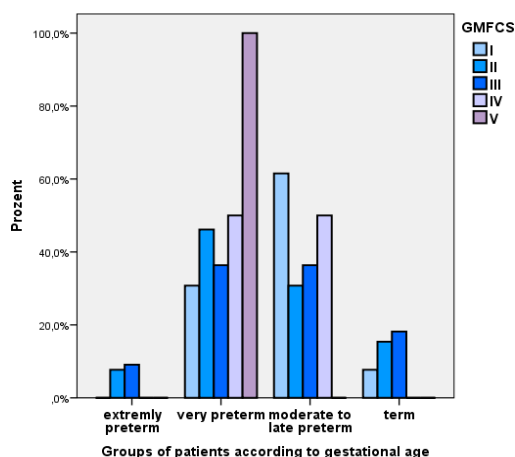


FIG. 22. Distribution of severity of GMFCS according to groups of gestational age.

4.2.2 Correlation between GMFCS Level and Age at MRI examination:

We did not find a significant correlation between the corrected age at which the MRI was carried out and the severity of cerebral palsy. In patients with least severity of CP (level I), the mean age at which the MRI was carried out, was with 99,92 months (SD 56,17) relative late in comparison to the other patients.

Tab. 12. Descriptive statistical of age at the time of MRI by GMFCS						
Age at the time of MRI (months)	total	GMFCS I	GMFCS II	GMFCS III	GMFCS IV	GMFCS V
N	50	13	13	11	10	3
Mean	69,66	99,92	49,92	60,73	65,7	70
Median	46	86	28	37	35	33
Min.	12	30	14	16	12	12
Max.	212	212	180	178	202	165
SD	60,17	56,17	50,91	54,12	72,54	82,94
r and p	$r=-0,14$ $p=0,29$					

4.2.3 Correlation between GMFCS Level and MRI-findings:

4.2.3.1 Study of Corpus Callosum:

4.2.3.1.1 Study of Length of Corpus Callosum:

The relationship between the severity of CP and the ratio of length of the corpus callosum to the anterior-posterior diameter of the skull (Min. 0,26, Max. 0,4, Mean 0,34, SD 0,36) shows moderately significant negative correlation with the increasing severity of CP with significant difference between GMFCS level V ($0,27 \pm 0,21$) and GMFCS level I ($0,35 \pm 0,26$) (FIG.23).

Tab. 13. Descriptive statistic of severity of cerebral palsy by length of corpus callosum						
Length of Corpus callosum (cm) /anterior-posterior diameter of skull (cm)						
	Total	GMFCS I	GMFCS II	GMFCS III	GMFCS IV	GMFCS V
N	50	13	13	11	10	3
Minimal	0,26	0,32	0,27	0,29	0,26	0,26
Maximal	0,40	0,40	0,38	0,40	0,38	0,30
Mean	0,34	0,35	0,33	0,34	0,32	0,27
Median	0,33	0,34	0,33	0,35	0,32	0,27
SD	0,04	0,03	0,03	0,04	0,03	0,02
95% CI		0,34-0,37	0,32-0,36	0,32-0,37	0,30-0,34	0,23-0,33
r and p	$r= -0,43$ $p <0,001$					

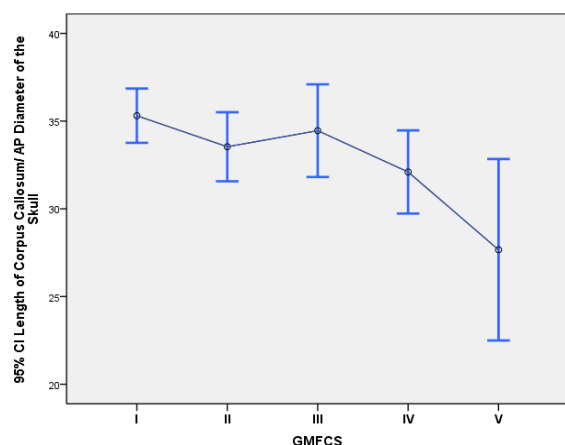


FIG. 23. Ratio of length of corpus callosum (95% CI) to AP diameter of the skull by GMFCS.

4.2.3.1.2 Study of Genu of CorpusCallosum:

The relationship between the severity of CP and the ratio of thickness of the genu to the anterior-posterior diameter of skull X 10 (Min. 0,06, Max.0,68, Mean 0,45, SD 0,15) shows moderately significant negative correlation with the increasing severity of CP. We have also found that ratio of thickness of the genu to AP diameter of the skull in GMFCS level IV group ($0,31 \pm 0,17$) is significantly smaller than in GMFCS I ($0,55 \pm 0,06$)(FIG.24).

Tab. 14. Descriptive statistic of severity of cerebral palsy by thickness of genu						
Thickness of genu (mm)/ anterior-posterior diameter of skull (mm) X10						
	Total	GMFCS I	GMFCS II	GMFCS III	GMFCS IV	GMFCS V
N	50	13	13	11	10	3
Minimal	0,06	0,46	0,10	0,36	0,06	0,29
Maximal	0,68	0,67	0,68	0,61	0,53	0,39
Mean	0,45	0,55	0,45	0,50	0,31	0,35
Median	0,49	0,56	0,48	0,52	0,3	0,38
SD	0,15	0,06	0,16	0,09	0,17	0,06
r and p	$r = -0,50$ $p < 0,001$					

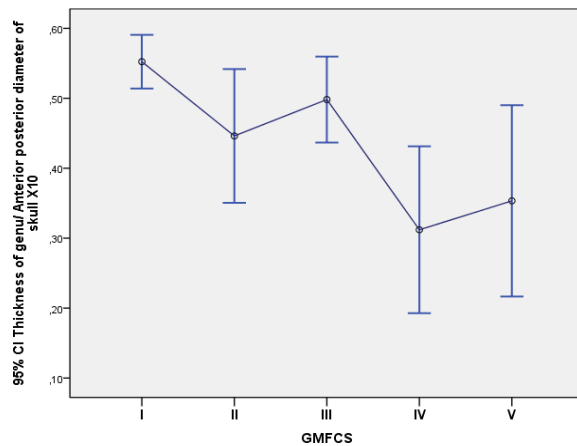


FIG.24. Ratio of thickness of the genu to the AP diameter of skull X 10 (95% CI) by GMFCS.

4.2.3.1.3 Study of Thickness of thinnest Part of Corpus Callosum:

The relationship between the severity of CP and thickness of the thinnest part of the corpus callosum (Min.0,5, Max.4,5, Mean 1,89, SD 0,88) shows moderately significant negative correlations with the increasing severity of CP.

The mean thickness of the thinnest part of the corpus callosum showed a gradual decrease with the increasing severity of CP (Tab.15). We have also found that the thickness of the thinnest part of the corpus callosum in GMFCS level I groups ($2,46 \pm 0,59$) is significantly greater than in GMFCS III ($1,68 \pm 0,56$) and IV groups ($1,35 \pm 0,78$)(FIG.26).

Tab. 15. Descriptive statistic of GMFCS by thickness of the thinnest part of corpus callosum

Thickness of the thinnest part of Corpus callosum (mm)						
	Total	GMFCS I	GMFCS II	GMFCS III	GMFCS IV	GMFCS V
N	50	13	13	11	10	3
Minimal	0,5	1,5	0,5	1	0,5	0,5
Maximal	4,5	3	4,5	2,5	3	2
Mean	1,89	2,46	2,04	1,68	1,35	1,33
Median	2	2,50	2,00	1,50	1,00	1,50
SD	0,88	0,59	1,11	0,56	0,78	0,76
95% CI		2,10-2,82	1,37-2,71	1,31-2,06	0,79-1,91	-,56-3,23
r and p	$r = -,48$ $p < 0,001$					

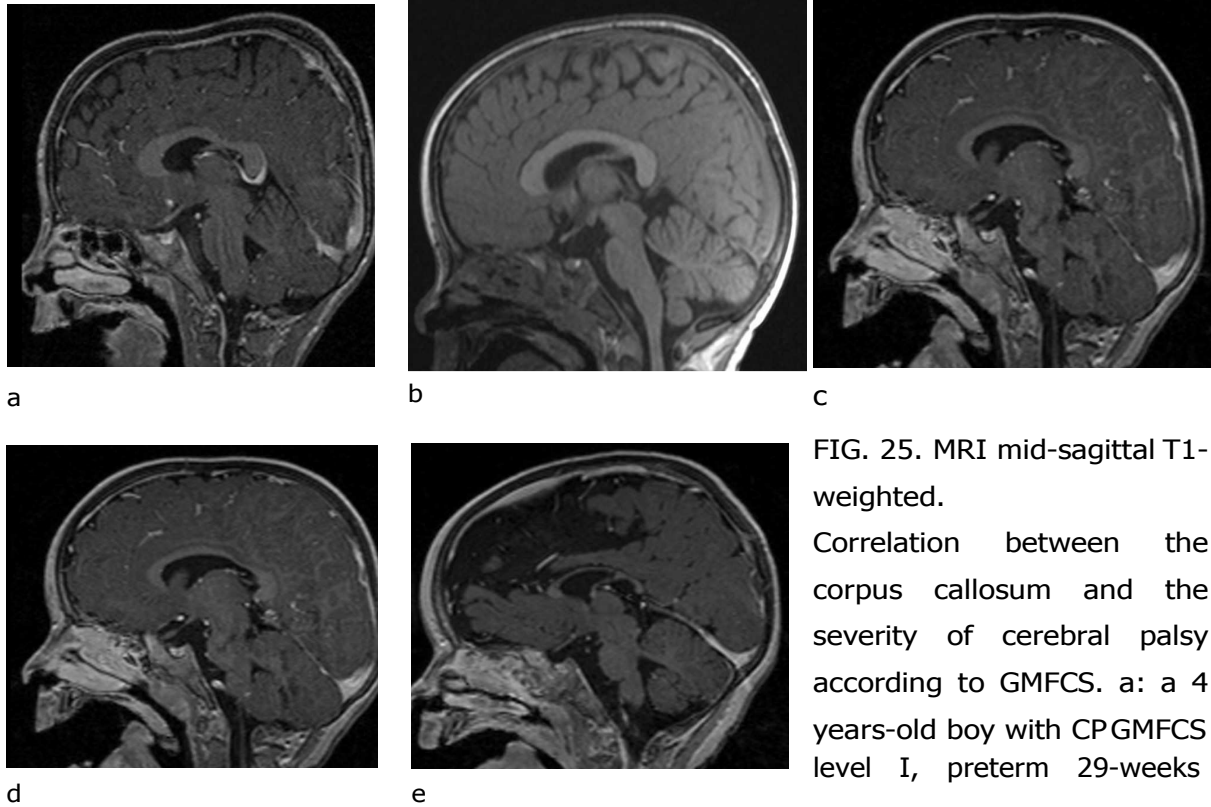


FIG. 25. MRI mid-sagittal T1-weighted.

Correlation between the corpus callosum and the severity of cerebral palsy according to GMFCS. a: a 4 years-old boy with CPGMFCS level I, preterm 29-weeks infants. b: 2 years-old girl with CP GMFCS level II, she

was born at 28 weeks. c: 2 years-old boy with CP GMFCS level III, he was 28 weeks preterm. d: 5 years-old girl with CP GMFCS level IV, e: 3 years-old boy with CP GMFCS level V. Note that the corpus callosum is fully developed at all levels of CP according to GMFCS. It is especially thinner in patients at levels IV and V of GMFCS.

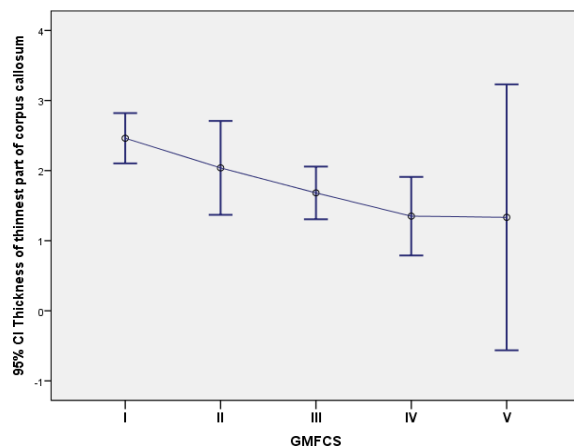


FIG. 26. Thickness of the thinnest part of corpus callosum (95% CI) by GMFCS.

4.2.3.1.4 Study of Location of thinnest Part of Corpus Callosum:

The focal thinning of corpus callosum in our study is almost always (92%) present at the junction between the body of corpus callosum and splenium (isthmus). In

58% present at posterior midbody of corpus callosum and in 32% at the anterior midbody of corpus callosum. We have also noticed that the thinnest part of corpus callosum is located in all patients with CP severity V at isthmus, posterior and anterior midbody, and in CP severity IV 70% of patients have atrophy at posterior midbody (FIG.27).

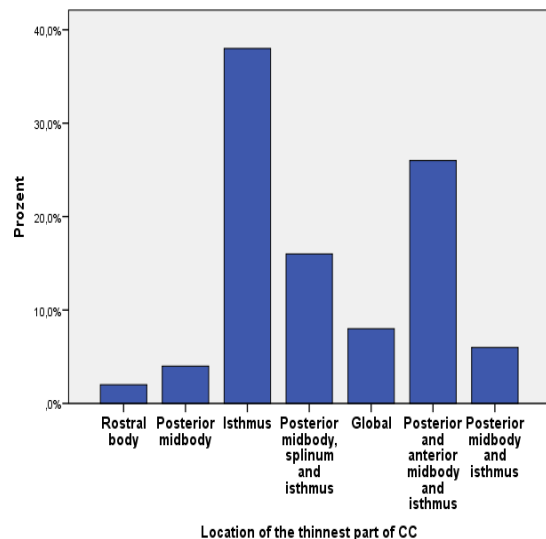


FIG. 27. Distribution of location of thinnest part of corpus callosum

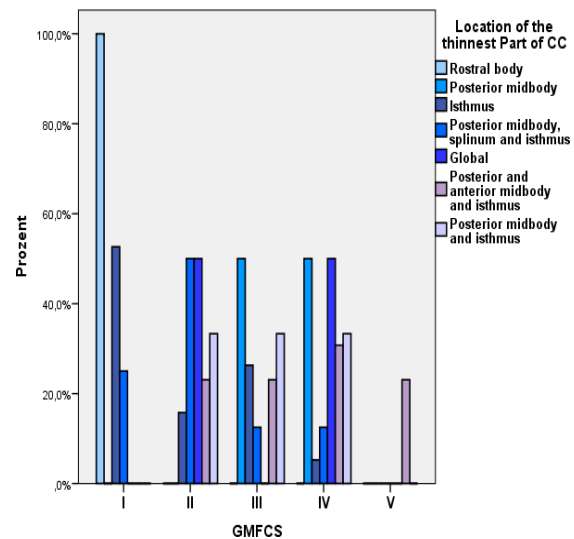


FIG. 28. Distribution of location of thinnest part of corpus callosum by patients with CP according to GMFCS

Tab.16. Location of the thinnest part of CC in patients with CP							
Location of the thinnest part of CC	GMFCS I n=13	GMFCS II n=13	GMFCS III n=11	GMFCS IV n=10	GMFCS V n=3	total n=50	Percent 100%
Rostral body	1	0	0	0	0	1	2%
Posterior midbody	0	0	1	1	0	2	4%
Isthmus	10	3	5	1	0	19	38%
Isthmus and posterior midbody	0	1	1	1	0	3	6%
Isthmus, posterior and anterior midbody	0	3	3	4	3	13	26%
Isthmus, posterior midbody and splenium	2	4	1	1	0	8	16%
Global	0	2	0	2	0	4	8%
r and p	r= 0,51				p <0,001		

4.2.3.1.5 Study of Correlation between all Parameters of Corpus Callosum:

We have found a significant moderately positive correlation between length of corpus callosum and the thickness of genu ($r=0,59, p <0,001$), between length of corpus callosum and the thickness of thinnest part of corpus callosum ($r=0,50, p <0,001$) and between thickness of genu and thickness of thinnest part of corpus callosum ($r=0,65, p <0,001$)(FIG.29).

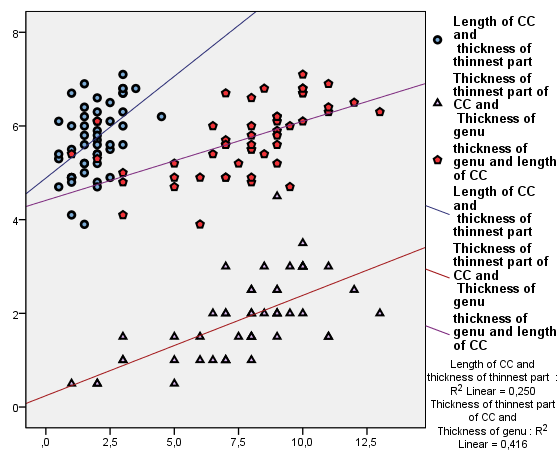


FIG.29. Scatter plot of length of corpus callosum and thickness of thinnest part of of corpus callosum, thickness of genu and length of corpus callosum, thickness of thinnest part of corpus callosum and thickness of genu

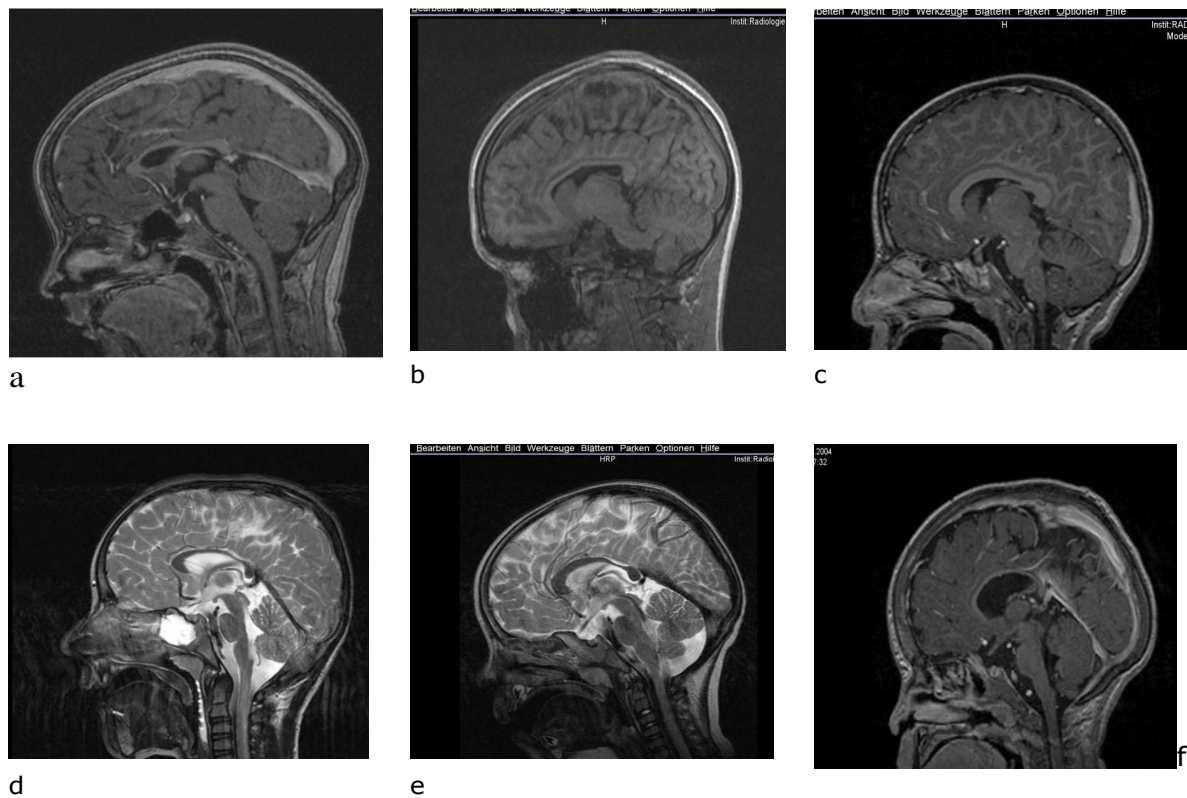


FIG.30. MRI show location of thinnest part of corpus callosum. a.: 11 years old girl with GMFCS I, she was a premature infant at 36 weeks. Note that the thinning of CC is at rostral body. b.: 15 years old girl with CP GMFCS level III, she was born at 32 weeks, she has also speech delay. Note that the thinning of the CC is at posterior midbody. c: 10 years old girl with GMFCS I, she was premature 29 weeks. Note the thinning of the CC at isthmus. d: 14 years old girl with CP GMFCS level IV, she was 31 weeks preterm infants, the thinning of CC is at the posterior midbody and isthmus. e: 5 years old boy with CP GMFCS level I, he was premature infants at 33 weeks, note that the thinning of the CC located at Isthmus, posterior midbody and splenium. f: 15 months old boy with CP GMFCS level IV, he was twins 34 weeks. Note that the thinning of CC is global.

4.2.3.2 Study of Brainstem:

4.2.3.2.1 Study of Midbrain:

We did not find a significant correlation or significant difference with the ratio of axial diameter of midbrain to the AP diameter of the skull X10 (Min. 0,51, Max.1,06, Mean 0,75, SD 0,1) by GMFCS (FIG.31).

Tab.17. Descriptive statistic of ratio of axial diameter of midbrain(mm) /anterior posterior diameter of skull (mm) X10 by GMFCS						
Ratio of diameter of midbrain axial (mm)/anterior posterior diameter of skull (mm)X10	Total	GMFCS I	GMFCS II	GMFCS III	GMFCS IV	GMFCS V
Number	50	13	13	11	10	3
Minimal	0,51	0,61	0,55	0,63	0,58	0,51
Maximal	1,06	1,06	0,93	0,9	0,88	0,7
Mean	0,75	0,77	0,74	0,77	0,74	0,62
Median	0,75	0,76	0,74	0,77	0,76	0,66
SD	0,1	0,12	0,1	0,08	0,08	0,1
r and p	r=-0,21 p=0,14					

We have found a significant moderate negative correlation between the ratio of diameter of midbrain sagittal to anterior posterior diameter of skull X10 (Min. 0,47, Max. 0,76, Mean 0,62, SD 0,06) and GMFCS without a significant difference between GMFCS groups (FIG.32).

Tab.18. Descriptive statistic of ratio of sagittal diameter of midbrain(mm) /anterior posterior diameter of skull (mm) X10 by GMFCS						
Ratio of diameter of midbrain sagittal (mm)/ anterior posterior diameter of skull (mm)X10	Total	GMFCS I	GMFCS II	GMFCS III	GMFCS IV	GMFCS V
Number	36	10	8	8	7	3
Minimal	0,47	0,56	0,55	0,55	0,47	0,57
Maximal	0,76	0,76	0,64	0,71	0,64	0,60
Mean	0,62	0,67	0,61	0,62	0,58	0,59
Median	0,62	0,68	0,62	0,60	0,57	0,59
SD	0,06	0,57	0,03	0,06	0,06	0,02
95% CI		0,62-0,71	0,58-0,63	0,57-0,67	0,52-0,64	0,55-0,62
r and p	r=-,48 p<0,001					

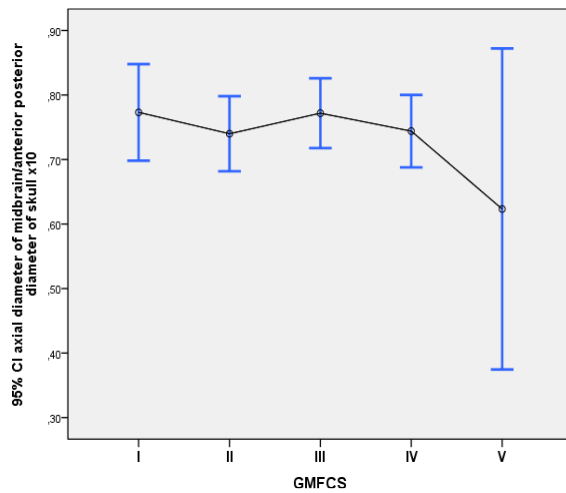


FIG. 31. Mean ratio of diameter of midbrain axial to AP diameter of skull X10 by GMFCS (95% CI)

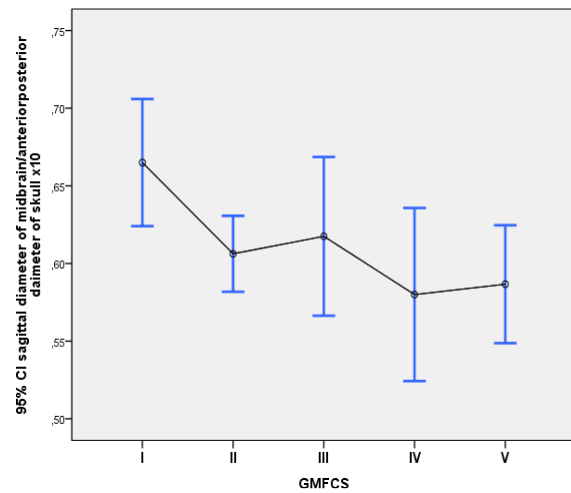
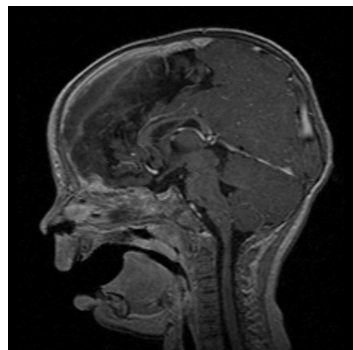


FIG. 32. Mean ratio of diameter of midbrain sagittal to AP diameter of skull X10 by GMFCS (95% CI)



a



b

FIG.33. MRIT1-sagittal show the atrophy of midbrain according to GMFCS. a.5 years old boy with CP severity I, note the full developed midbrain. b.1 year old boy with CP severity V, note the atrophy of the midbrain.

4.2.3.2.2 Study of Cerebral Peduncles:

There is a significant moderate negative correlation between the severity of CP and the ratio of axial diameter of both cerebral peduncles (Min. 0,11, Max. 0,17, Mean 0,14, SD 0,01) to AP diameter of skull without a significant difference between GMFCS groups (FIG.34).

Tab.19. Descriptive statistic of ratio of axial diameter of cerebral peduncles (mm)/ AP diameter of skull (mm) by GMFCS

Ratio of axial diameter of cerebral peduncles / AP diameter of skull	Total	GMFCS I	GMFCS II	GMFCS III	GMFCS IV	GMFCS V
Number	46	11	11	11	10	3
Minimal	0,11	0,14	0,12	0,13	0,12	0,11
Maximal	0,17	0,16	0,16	0,17	0,16	0,13
Mean	0,14	0,15	0,14	0,15	0,14	0,12
Median	0,14	0,15	0,14	0,14	0,14	0,13
SD	0,01	0	0,01	0,01	0,01	0,01
r and p	r=-,41 p<0,05					

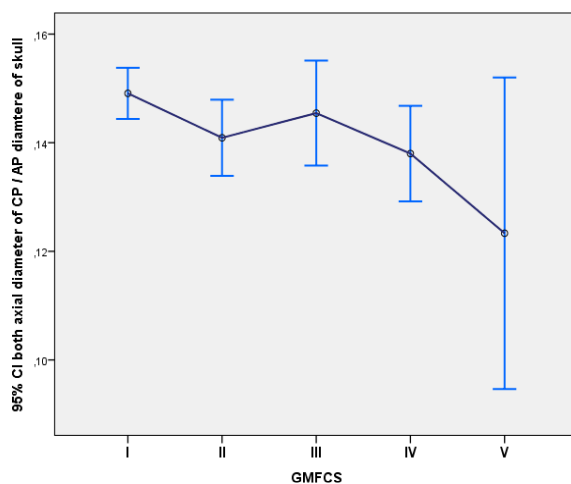


FIG.34. Mean ratio of axial diameter of cerebral peduncles to AP diameter of skull (95% CI) by GMFCS

4.2.3.2.3 Study of Pons:

We have not found a significant correlation between the severity of CP and the ratio of craniocaudal diameter of pons (Min. 0,07, Max.0,16, Mean 0,13, SD 0,02) to AP diameter of skull. We did not find a significant difference in this ratio between GMFCS- Level groups. The mean ratio of craniocaudal diameter of pons to AP diameter of skull shows a decrease in the mean value between GMFCS II and GMFCS III (FIG.35).

Tab.20. Descriptive statistic of ratio of craniocaudal diameter of pons (mm) to AP diameter of skull (mm) by GMFCS

Ratio of craniocaudal diameter of Pons to AP diameter of skull	Total	GMFCS I	GMFCS II	GMFCS III	GMFCS IV	GMFCS V
Number	46	11	11	11	10	3
Minimal	0,07	0,12	0,12	0,11	0,07	0,10
Maximal	0,16	0,15	0,14	0,14	0,16	0,14
Mean	0,13	0,13	0,13	0,12	0,12	0,12
Median	0,12	0,13	0,13	0,12	0,13	0,11
SD	0,02	0,01	0,01	0,01	0,03	0,02
95% CI		0,12-0,14	0,12-0,13	0,12-0,13	0,11-0,14	0,07-0,17
r and p	r=-,20 p=,17					

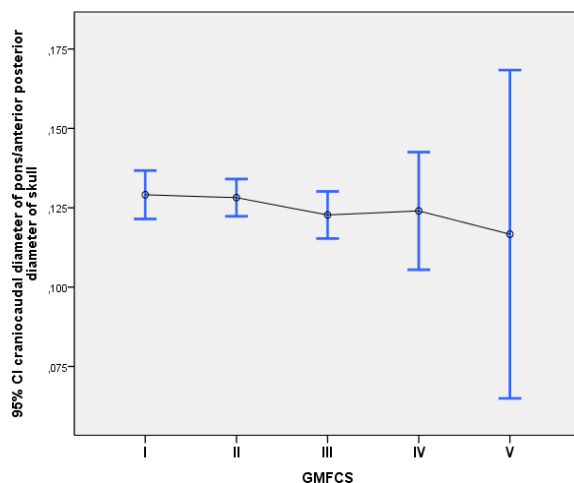


FIG.35. Mean ratio of craniocaudal diameter of pons axial to AP diameter of skull by GMFCS (95% CI)

4.2.3.3 Study of Lateral Ventricles:

4.2.3.3.1 Study of Grade of Extension of Lateral Ventricles:

We have found a significant positive moderate correlation between the grade of extension of lateral ventricles (Skala I-V) and GMFCS.

There was a clearly increase in the mean grade of extension of lateral ventricle between CP level I (Min 1, Max 3) and CP level IV (Min. 2, Max. 5) (Tab.21) with significant difference between GMFCS I and IV (FIG.37). At severity III of CP on we have beginning to find grade IV of LV-Extension and at severity IV of cerebral palsy on we have beginning to find grade V of LV- Extension (FIG.36).

Tab.21. Descriptive statistic of grade of extension of lateral ventricle by GMFCS						
Grade of extension of lateral ventricle	Total n=50	GMFCS I n=13	GMFCS II n=13	GMFCS III n=11	GMFCS IV n=10	GMFCS V n=3
Minimal	1	1	1	1	2	1
Maximal	5	3	3	4	5	5
Mean	2,18	1,54	1,77	2,36	3,2	2,67
Median	2	1	2	2	3	2
SD	1,16	0,66	0,83	1,03	1,23	2,08
r and p	r= 0,5 p <0,001					

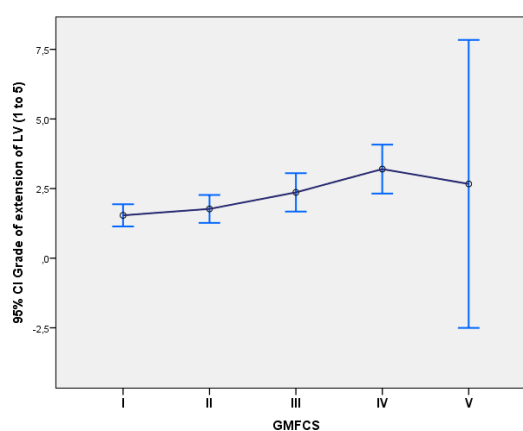
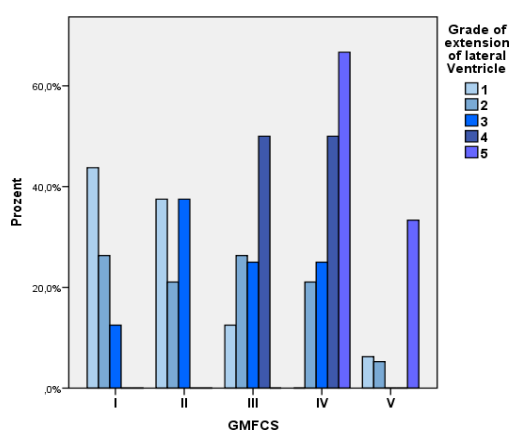


FIG.36. Distribution of grade of extension of LV according to severity of CP

FIG.37. Mean grade of extension of lateral ventricle (95% CI) by GMFCS

4.2.3.3.2 Study of Width of Posterior Horn of Lateral Ventricles:

We have found a significant positive moderate correlation between the ratio of width of both posterior horn of lateral ventricle/AP diameter of skull and GMFCS (Tab.22).

There was also a significant difference in the mean ratio of width of posterior horn / AP diameter of skull between GMFCS levels I ($0,1 \pm 0,03$) and GMFCS level IV ($0,16 \pm 0,04$) (FIG.38).

Tab.22. Descriptive statistic of ratio of width of posterior horn of lateral ventricle (mm) to AP diameter of skull (mm) by GMFCS

Ratio of width of both posterior horns of lateral ventricle/ AP diameter of skull	Total n=50	GMFCS I n=13	GMFCS II n=13	GMFCS III n=11	GMFCS IV n=10	GMFCS V n=3
Minimal	0,05	0,06	0,05	0,08	0,12	0,07
Maximal	0,25	0,15	0,20	0,22	0,24	0,25
Mean	0,13	0,10	0,12	0,14	0,16	0,14
Median	0,13	0,10	0,14	0,13	0,16	0,11
SD	0,05	0,03	0,05	0,04	0,04	0,09
95% CI		0,08-0,12	0,09-0,15	0,11-0,17	0,14-0,19	-0,09-0,38
r and p	r= 0,44 p <0,001					

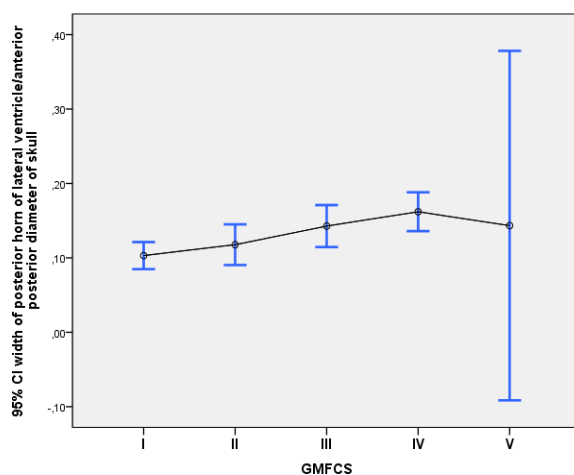


FIG.38. Mean ratio of width of posterior horn of lateral ventricle to AP diameter of skull (95% CI) by GMFCS

4.2.3.3.3 Study of Depth of Extraction of Lateral Ventricle:

We have found a significant positive moderate correlation between the depth of extraction of lateral ventricle on both sides and GMFCS.

The mean depth of extraction of the lateral ventricle (Min. 0, Max. 9, Mean 3,37. SD 2,38) increases with GMFCS levels on both sides between level I and IV (Tab.23). This diameter was significantly smaller in GMFCS level I ($1,78 \pm 1,79$) than in GMFCS level IV ($5,45 \pm 2,6$) and V ($5,17 \pm 0,29$) and in GMFCS level II ($2,58 \pm 2,23$) than in level V ($5,17 \pm 0,29$) (FIG.39).

4.2.3.3.4 Study of Distance between Lateral Ventricle and Cortex:

Whereas there was a significant moderate negative correlation between the severity of cerebral palsy and the distance between lateral ventricle and cortex, this distance was significantly greater in GMFCS level I group ($6,15 \pm 2,3$) than in GMFCS level III ($2,91 \pm 2,28$) and IV ($1,6 \pm 3,24$) (FIG.40). However the mean of this distance (Min.0, Max. 13) decreases steadily with the increasing severity of the cerebral palsy (Tab.24).

Tab.23. Descriptive statistic of depth of extraction of lateral ventricle (mm) by GMFCS level

Depth of the extraction of lateral ventricle on both sides	Total n=50	GMFCS I n=13	GMFCS II n=13	GMFCS III n=11	GMFCS IV n=10	GMFCS V n=3
Minimal	0	0	0	1	0	5
Maximal	9	4	7	6	9	5,5
Mean	3,37	1,78	2,58	3,82	5,45	5,17
Median	3,5	2	2	4	5	5
SD	2,38	1,79	2,23	1,47	2,6	0,29
95% CI		0,70-2,87	1,23-3,93	2,83-4,81	3,59-7,31	4,45-5,88
r and p	r= 0,57 p <0,001					

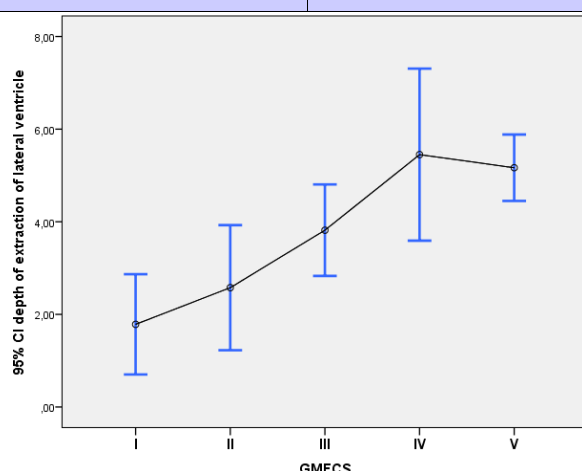


FIG. 39. Mean depth of extraction of lateral ventricle (95%CI) by GMFCS

Tab.24. Descriptive statistic of distance between lateral ventricle and cortex (mm) by GMFCS

Distance between lateral ventricle and cortex	Total n=50	GMFCS I n=13	GMFCS II n=13	GMFCS III n=11	GMFCS IV n=10	GMFCS V n=3
Minimal	0	4	0	0	0	0
Maximal	13	13	6	7	10	3
Mean	3,5	6,15	3,3	2,91	1,6	1,33
Median	3,5	6	4	2	0	1
SD	3	2,3	2,59	2,28	3,24	1,53
r and p	r=-0,54 p<0,001					

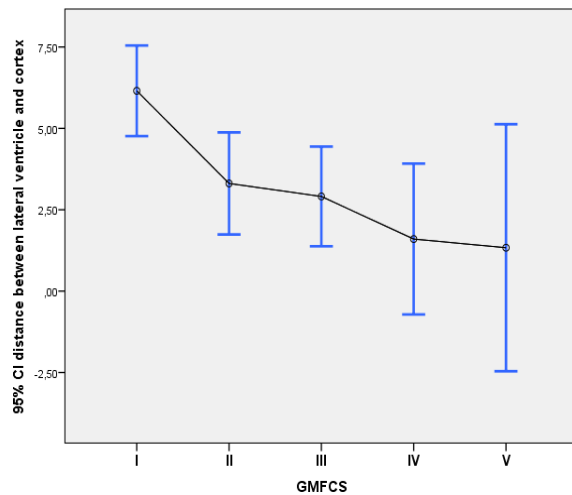


FIG.40. Mean distance between lateral ventricle and cortex (95% CI) by GMFCS

4.2.3.3.5 Study of Distance between Extraction of Lateral Ventricle and Cortex:

The distance between the extraction of LV and the cortex show no significant correlation (FIG.41) with the GMFCS level (Tab.25).

Tab.25. Descriptive statistic of distance between extraction of lateral ventricle (mm) by GMFCS

Distance between the extraction of LV and cortex	Total n=48	GMFCS I n=13	GMFCS II n=12	GMFCS III n=10	GMFCS IV n=10	GMFCS V n=3
Minimal	0	0	0	3	0	8
Maximal	25	25	22	25	14	11
Mean	8,75	8,27	9,83	10,1	6,35	10
Median	9	9	10,5	8,25	6	11
SD	6,54	8,88	6,11	6,48	4,42	1,73
r and p	r= -0,04 p=0,77					

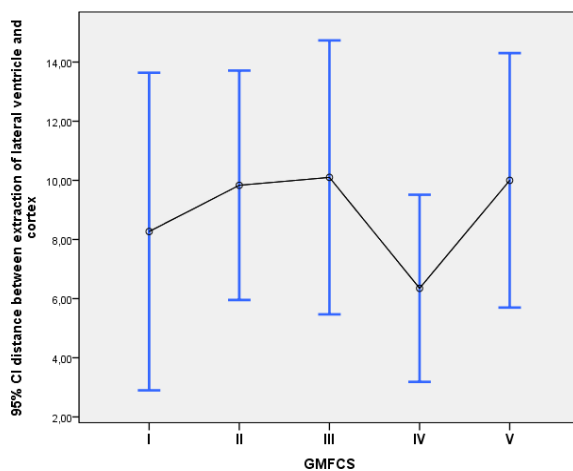


FIG.41. Distance between extraction of lateral ventricle and cortex by GMFCS (95% CI)

4.2.3.4 Study of Gliosis:

4.2.3.4.1 Study of Grade of Gliosis:

We did not find a significant correlation between the grade of gliosis (Min. 2, Max. 5, Mean 3,1, SD 1,04) and the severity of cerebral palsy (Tab.26).

Tab.26. Descriptive statistic of grade of gliosis by GMFCS						
Grade of gliosis	Total n=50	GMFCS I n=13	GMFCS II n=13	GMFCS III n=11	GMFCS IV n=10	GMFCS V n=3
Minimal	2	2	2	2	2	2
Maximal	5	4	5	4	5	5
Mean	3,1	2,62	3,38	2,73	3,6	3,67
Median	3	2	3	3	4	4
SD	1,04	0,87	1,04	0,79	1,08	1,53
r and p	r= 0,27 p= 0,06					

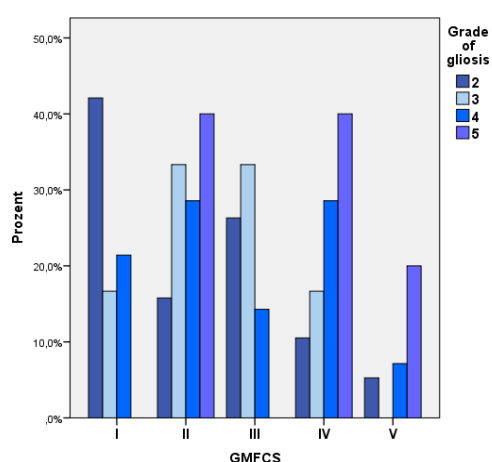


FIG.42. Distribution of grade of gliosis according to severity of CP

4.2.3.4.2 Study of Width of Gliosis:

We did not find a significant correlation between the width of gliosis and the severity of cerebral palsy (Tab.27).

Tab.27. Descriptive statistic of width of gliosis on both sides (mm) by GMFCS						
Width of the gliosis	Total n=50	GMFCS I n=13	GMFCS II n=13	GMFCS III n=11	GMFCS IV n=10	GMFCS V n=3
Minimal	4	8	11,5	8	4	6
Maximal	33	26	33	22	29	26
Mean	16,56	13,77	19,23	14,27	18,9	17,67
Median	14,5	12	19	14	19	21
SD	7,21	6,85	7,09	4,5	8,52	10,41
r and p	r=0,15 p=0,29					

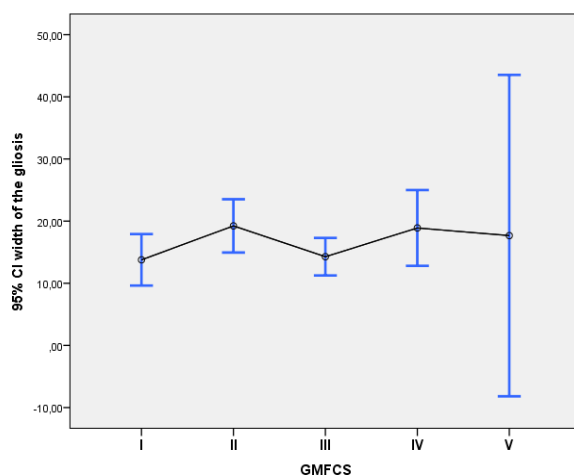


FIG.43. Width of gliosis by GMFCS (95% CI)

4.2.3.4.3 Study of the Distance between Gliosis and Cortex:

The correlation between the severity of CP and distance between gliosis and cortex (Min. 0, Max. 20,5, Mean 3,05, SD 3,56) was significant moderate negative correlation (Tab.28). At level V of CP was the distance in all cases 0. The mean distance shows a gradual decrease with the increasing severity of cerebral palsy with a slight increase between level II and III. This distance was significantly smaller in GMFCS level V (0) group than in GMFCS level I, II and III groups (FIG.44).

Tab.28. Descriptive statistic of distance between gliosis and cortex (mm) by GMFCS						
Distance between gliosis and cortex	Total n=50	GMFCS I n=13	GMFCS II n=13	GMFCS III n=11	GMFCS IV n=10	GMFCS V n=3
Minimal	0	0	0	0	0	0
Maximal	20,5	20,5	10	6	6	0
Mean	3,05	5,62	2,81	2,86	1,15	0
Median	2,75	4,5	3	3	0	0
SD	3,56	5,09	2,91	1,52	1,92	0
r and p	r= -0,46 p=0,001					

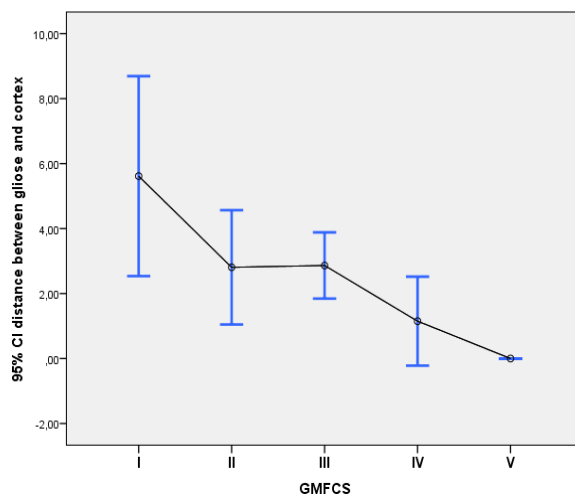


FIG.44. Mean distance between gliosis and cortex (95% CI) by GMFCS

4.2.3.5 Small Porencephalic Cysts in MRI (“black holes”):

17 patients (34%) in our study have black holes (i.e small porencephalic cysts) (FIG.45).

We have not found a significant correlation between the severity of cerebral palsy and the existence of small porencephalic cysts on MRI ($r=0,12$, $p= 0,17$). At level IV of cerebral palsy the frequency of patients with black holes on MRI was with 70% the highest among the patients (Tab.29).

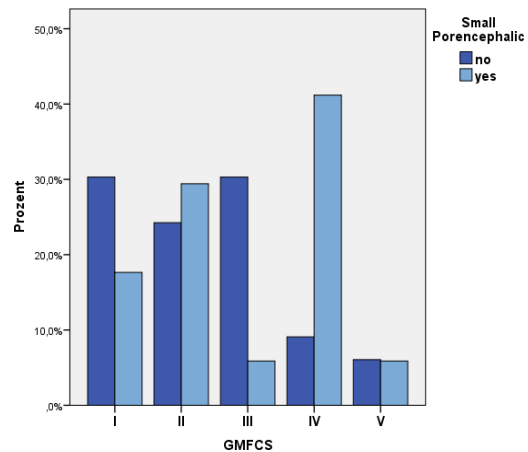
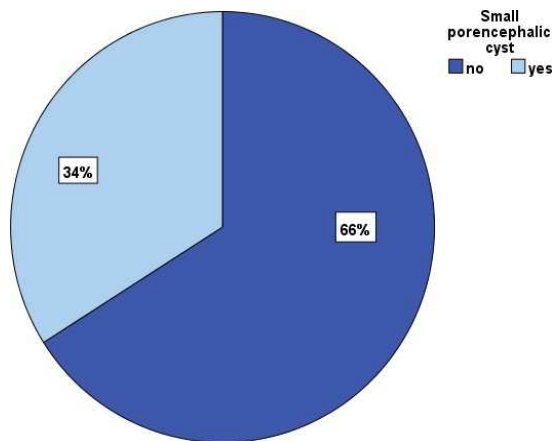


FIG.45. Existence of small porencephalic cysts in our study

FIG.46. Distribution of small porencephalic cysts according to GMFCS

Tab.29. Descriptive statistic of existence of small porencephalic cysts on MRI by GMFCS						
Small porencephalic cysts	Total n=50	GMFCS I n=13	GMFCS II n=13	GMFCS II n=11	GMFCS IV n=10	GMFCS V n=3
Mean	0,34	0,23	0,38	0,09	0,7	0,33
SD	0,48	0,44	0,5	0,3	0,48	0,58
r and p	r=0,20 p=0,17					

4.2.3.6 Microhemorrhages on T2*-weighted gradient echo MRI:

3 patients in our study (11%) have microhemorrhage on T2*-weighted gradient echo MRI. 2 patients of them have CP level IV and 1 patient has CP level III (Tab.30).

Tab.30. Descriptive statistic of existence of microhemorrhages on T2*-Weighted MRI by GMFCS						
Existence of hemorrhage on T2*-weighted GER	Total n=27	GMFCS I n=4	GMFCS II n=8	GMFCS III n=7	GMFCS IV n=6	GMFCS V n=2
yes	3	0	0	1	2	0
no	24	4	8	6	4	2
SD	0,32	0	0	0,3	0,42	0
r and p	r=,27 p=0,17					

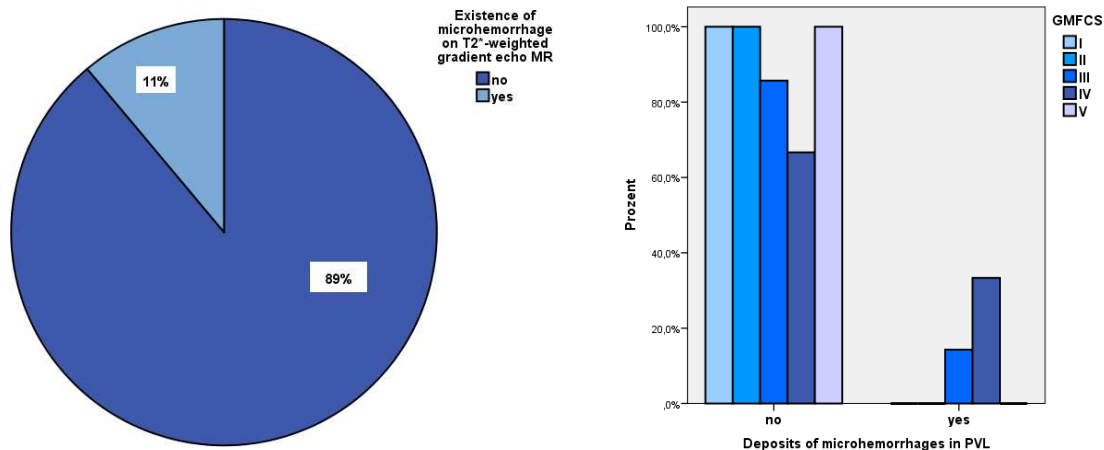


FIG.47. Existence of microhemorrhages on T2*-weighted gradient echo MR in our study

FIG.48. Existence of microhemorrhages on T2*-weighted gradient echo MR according to severity of cerebral palsy

4.2.4 Correlation between left and right of MRI-findings:

We have found a highly significant positive correlation between the left and right findings of MRI in the patients in our study(FIG.49).

Correlation between right and left	total	r	p
Axial diameter of cerebral peduncles	46	0,91	<0,001
Extension of the posterior horn of the lateral ventricles	50	0,78	<0,001
Distance between Cortex and LV	49	0,96	<0,001
Distance between cortex and extension of LV	49	0,91	<0,001
Depth of the edge of LV extraction	50	0,83	<0,001
Width of gliosis	50	0,86	<0,001
Distance between gliosis and cortex	50	0,57	<0,001

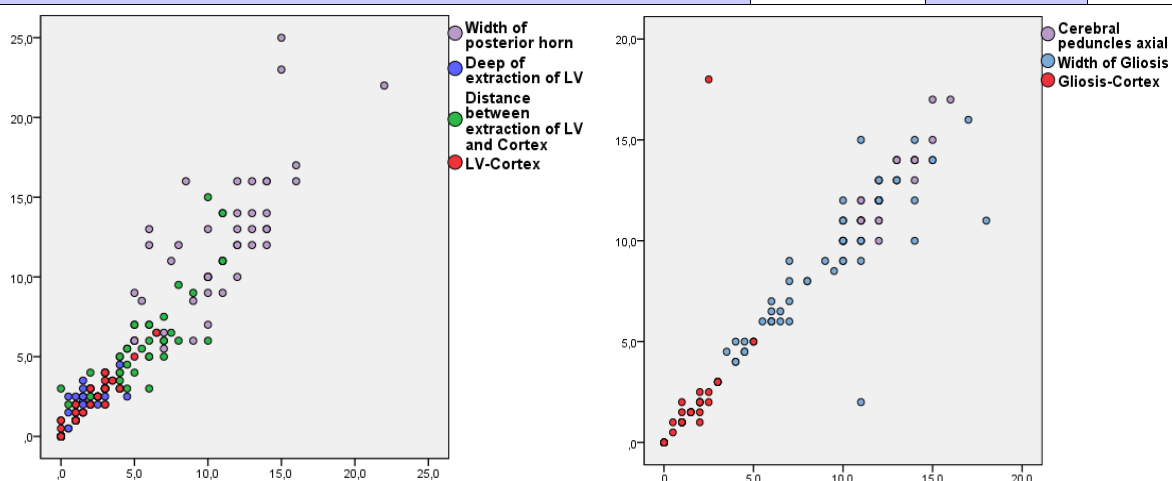


FIG.49. Scatter plots show correlation between right and left-findings on MRI

4.3 Subgroups Data of Patients according to gestational age:

45 (90%) of the participants were premature infants (gestational age less than 37 weeks) and 5 (10%) were born at term. Mean gestational age at birth was 31,8 weeks (SD 3,08 weeks), median 32 weeks (range: 26-39 weeks). We have found 2 patients (4%) with gestational age <28 weeks, 22 patients (44%) between 28 to < 32 weeks, 21 patients (42%) between 32 to < 37 weeks and 5 patients (10%) at the age ≥ 37 weeks (FIG.50).

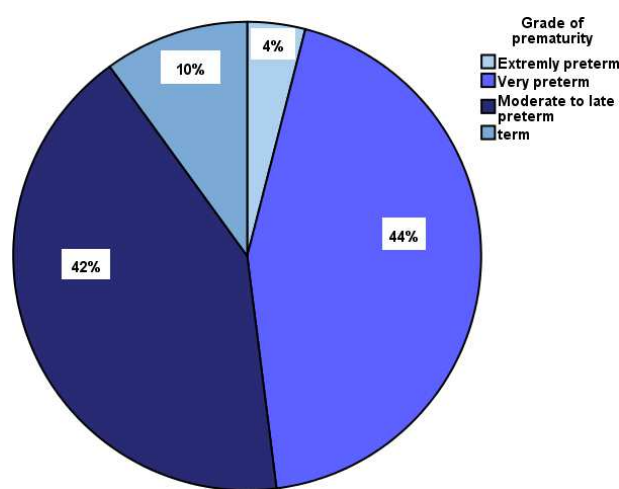


FIG.50. Distribution of patients according to gestational age

4.3.1 Correlation between Gestational age and MRI-findings:

4.3.1.1 Study of Corpus callosum:

We did not find any significant correlation between the following measurements of corpus callosum (length of corpus callosum/ anterior posterior diameter of skull, thickness of genu/ anterior posterior diameter of the skull X 10, thickness of thinnest part of corpus callosum) and gestational age at birth.

4.3.1.2 Study of Brainstem:

We did not find any correlation between the following measurements of brainstem (axial and sagittal diameter of midbrain /anterior posterior diameter of skull X 10, craniocaudal diameter of pons/ anterior posterior diameter of skull X 10 and

diameter of cerebral peduncle on both sides/ anterior posterior diameter of skull) and gestational age at birth.

4.3.1.3 Study of lateral ventricle:

We did not find any correlation between gestational age at birth and all parameters of lateral ventricles. However grade V of extension of lateral ventricle exist only by preterm infants with gestational age 28 to < 32 weeks at birth.

4.3.1.4 Study of gliosis:

We did not find a correlation between the gestational age at birth and grade of gliosis and the distance between gliosis and cortex on both sides. However we have found a slight positive correlation between the width of gliosis on both sides and gestational age at birth.

4.3.1.5 Small Porencephalic cysts in MRI ("black holes"):

The existence of porencephalic cysts (mean 0,34, SD 0,48) achieves its peak between 32 to < 37 gestational weeks at birth.

4.3.1.6 Microhemorrhages on T2*-weighted gradient echo MRI:

The 3 patients (11%) who have microhemorrhages on T2*-weighted gradient-echo MR images were premature infants between 28 to < 32 gestational weeks at birth.

Tab. 32. Correlation between Gestational age and MRI-findings		<i>r</i>	<i>p</i>
Study of corpus callosum	Length of CC/anterior posterior diameter of the skull	-0,14	0,34
	Thickness of genu/ anterior posterior diameter of the skull X 10	-0,12	0,4
	Thickness of thinnest part of CC	-0,12	0,41
Study of Brainstem	Axial diameter of midbrain/anterior posterior diameter of the skull X10	0,21	0,15
	Sagittal diameter of midbrain/anterior posterior diameter of the skull X10	0,27	0,11
	Sagittal craniocaudal diameter of pons/anterior posterior diameter of the skull X 10	0,1	0,48
	Diameter of cerebral peduncle on both sides/anterior posterior diameter of the skull	0,2	0,18
Study of lateral ventricles	Grade of LV- extension	0,14	0,32
	Distance between LV on both sides and cortex	0,01	0,96
	Distance between extraction of LV on both sides and cortex	-0,13	0,4
	Width of posterior horn on both sides/anterior posterior diameter of the skull	-0,14	0,32
	Depth of extraction of LV on both sides	-0,2	0,17
Study of gliosis	Grade of gliosis	-0,16	0,28
	Width of gliosis on both sides	0,29	<0,05
	Distance between gliosis on both sides and cortex	-0,19	0,19
Study of porencephalic cysts		0,1	0,48
Study of Microhemorrhages on T2*-weighted gradient echoMRI		-0,16	0,44

5. Discussion:

It is proposed that structural MRI should be considered to clarify the association between brain morphology and function qualitative and quantitative approaches^(92,94).

5.1 Total Cohort:

Until now, there is a lack of valid tools for assessing brain lesions severity and its correlation to the severity of function deficit in patients with CP⁽⁹²⁾.

In a recent study from (Fiori et al.,2015)⁽⁹²⁾, they tried to develop a semi-quantitative MRI scale in children with CP due to PWM lesions. Their study included a subgroup of mild to moderately impaired children with CP with a cohort from 34 patients. In their study only children with Flair images were included. In our study, we have included all subgroups of mild, moderate to severe forms of CP with a cohort of 50 patients. We have tried to develop an easily applicable parameter which can be measured by using T2 weighted MRI sequences.

Since we expected a higher validity when the study oriented within a homogeneous patient-group, we have included purely patients with CP due to PWM. That could be a possible limitation of the present study, while it permits only a partial representation for the children with CP. Further studies in a larger cohort, and with different type of brain lesions are required.

To allow a wide age-independent application of the parameters, we have included individual with CP until age of 212 months, starting with 12 months when the brain has reached a good level of maturation ⁽⁹⁵⁾. For this reason, we have used the ratios of the parameters to the diameter of the skull, except for the depth of the extraction of lateral ventricles.

The most common severity grade of cerebral palsy in our patients was the level I and II with equal rate (26%). These results are in agreement with those of a study from (Beckung et al.,2000)⁽²³⁾, which showed that most of the children with cerebral palsy were classified according to GMFCS at level I and level II (38% and 22%

respectively). Level III in our study was with (22%) higher than that in the previous study (8%) and level V with (6%) was less common (15%). That could be due to the exclusion of the patients with hemorrhage and hydrocephalus, whom usually have more severity forms of CP.

Although there were no relations between the age at which the MRI was carried out and the severity of cerebral palsy, the mean age at the time of MRI was with (69,66 months) relative late, especially in patients with level I (99,92 months), that could be related to the low compliance of children under 6 years of age for MRI and the need to do it under anesthesia, which makes many parents refuse it.

5.2 GMFCS Level and MRI-findings:

To our knowledge, this study is the first to detect the depth of extraction of the lateral ventricle as a quantitative marker of the severity of motor impairment in children with BS-CP.

We have confirmed, the use of the depth of extraction of the lateral ventricle to distinguish between patients at GMFCS level I and IV, I and V and between II and V. We have also found a relevant difference in the grade of extension of LV between GMFCS levels I, II and GMFCS level IV.

The quantitative assessment of the mean ratio of width of the posterior horn/ AP diameter of the skull showed us with 95% CI a significant difference between patients with CP at GMFCS level I (0,08- 0,12%) and at GMFCS level IV (0,14- 0,19%).

We have also found a moderate significant negative correlation between the severity of cerebral palsy and the distance between lateral ventricle and cortex. However, we did not find any correlation between the distance between the extraction of LV and the cortex and the severity of CP.

It is interesting to know that, when the ratio of the length of the corpus callosum to the diameter of the skull by a patient with BS-CP is $\geq 0,34$ %; we can say with 95% confidence that he could not have GMFCS V. When this ratio is lower than 0,33% the patient had no GMFCS level I with 95% CI.

By measuring the mean of the thinnest part of the corpus callosum, we could differentiate between GMFCS level I and III and between GMFCS level I and IV. Further researches are needed to support our results and to find the difference in brain lesions at the other groups of GMFCS.

The focal thinning of the corpus callosum presents in (92%) of patients at the isthmus, in 58% at posterior midbody and in 32% at the anterior midbody of the corpus callosum which emphasized that the callosal motor fibers cross the corpus callosum in isthmus and posterior body. This finding is consistent with previous reports from (Wahl M. et al.,2007) ⁽⁶⁰⁾ and from (Hofer et al.,2006)⁽⁶¹⁾.

The anterior part of the corpus callosum (rostral body) which connects the prefrontal cortex was the least affected (2%) in our study (preterm 36 weeks, GMFCS level I), whereas the splenium which contains, fibers come from the visual and visual-association areas of the cortex, was in 16% affected in our study.

All the measurements of the corpus callosum show clear correlation with each other's, which suggested that the corpus callosum was completely atrophic. In all patients of this study, the corpus callosum was fully developed. It is known, that the formation of the corpus callosum completed by 18-20 gestational weeks. Since PVL is a white matter injury during the late second or the early third trimester of pregnancy, it could explain that in all patients of this study, the corpus callosum was fully developed but atrophic and emphasizes the hypotheses that the insult of the white matter has happened after the formation of the corpus callosum (i.e. after 20 gestational weeks)^(41, 62).

Following brain injury, MR imaging has detected tract changes. Within descending tracts at 4 weeks after the ischemic- insult T2-hypointensity was reported. Whereas after 10-14 weeks permanent T2-hyperintensity changes were observed followed by stem atrophy over months to years⁽⁶⁶⁾. In one study from (Lama et al.,2010) in neonatal rats with unilateral cerebral infarction, there was evidence for axonal changes in the first days to weeks following injury⁽⁶⁴⁾. It was demonstrated that post cerebral- ischemic insult in the neonatal brain a degeneration of the descending corticospinal tract, notably the cerebral peduncle, can be observed⁽⁶⁴⁾. In a recent study from (Domi et al., 2009) it was noticed an increase in intensity in

diffusion weighted images within the cerebral peduncle in patients with the poor outcome⁽⁶⁷⁾ after cerebral ischemic insult.

In our study, we have found a significant moderate negative correlation between the ratio of diameter of midbrain (sagittal) to the AP diameter of skull, diameter of cerebral peduncles and severity of cerebral palsy with no clear difference at the GMFCS-levels. We did not find a clear correlation with the axial diameter of midbrain.

As pons is a white matter tract transmit the motor fibers to the face and body⁽⁵⁸⁾, we consider the secondary degeneration of the cerebral white matter tracts, which happened in PVL, could result in pons hypoplasia⁽⁵⁶⁾. (Argyropoulou et al.,2003)⁽⁵⁷⁾ and (S. Yoshida et al.,2007)⁽⁵⁶⁾ have found that the AP diameter of the pons was significantly smaller in premature infants with PVL than in the control group. Our study showed no relevant correlation with the severity of CP.

In our study, we did not find a correlation between the severity of cerebral palsy and the grade of gliosis or between severity of CP and width of gliosis.

But, we have found a significant negative moderate correlation between the severity of CP and distance between gliosis and cortex. This distance was 0 by all patients with severity V of CP and was significantly smaller in GMFCS level V group than in GMFCS level groups (I, II, III) and significantly greater in GMFCS level I than in other groups.

Porencephalic cysts were detected in 34% of patients. They were observed more frequently at the level IV of cerebral palsy. However, there was no correlation between the presence of porencephalic cysts and increased severity of cerebral palsy.

There was no relation between the severity of CP and the existence of microhemorrhages on gradient-echo T2*-weighted MR images. However, the existence of microhemorrhage was more frequently at the level IV and III of CP.

We have found a highly significant positive correlation between the left and right findings of MRI in the patients in our study. A study from (Loukia et al.,2009)⁽⁸⁷⁾

showed that MRI-findings were bilateral and symmetric in all patients with PVL with increased gray matter volume in specific areas (putamen, thalamus, lingual gyrus, frontal superior gyrus and superior cingulate gyrus), decreased white matter volume and increased total CSF volume⁽⁸⁷⁾.

5.3 Gestational age:

In our study 90% of the participants were preterm infants, and 10% were born at term. This result does not contradict the idea that PVL is a form of hypoxic-ischemic damage of the immature brain, but it suggested that PVL in term infants may reflect a cerebral injury occurred in utero^(76, 77, 78). The largest number of patients (44%) were preterm infants born at the early 3rd trimester (28 to <32 gestational weeks). These results are in agreement with the studies of (Okumura et al., 1997)⁽⁷⁹⁾ who has reported that PVL is less likely to occur at the late third of the trimester.

The severity of cerebral palsy shows in our study no significant correlation with gestational age at birth. Whereas term infants show a slight to moderate form of cerebral palsy (I-III), patients with the highest form of severity (level V) were all born at the early stage of 3rd trimester (28 to < 32 weeks). A similar finding was observed in a study from (Okumura et al., 1997)⁽⁷⁹⁾ which indicated that PVL shows milder form in term infants than those born around early stage of 3rd trimester, indicating that brain injury in term infants, which may occur in utero, while it is less severe, does not result in preterm birth⁽⁷⁹⁾.

We have found a slight correlation between gestational age at birth and width of gliosis. Otherwise, we did not find any other correlation with the other MRI-findings (corpus callosum, midbrain, pons, cerebral peduncles, lateral ventricles, gliosis, small porencephalic cyst and microhemorrhage). These results are in agreement with (Melhem et al., 2000)⁽³⁹⁾ who has reported no correlation between gestational age and the lateral ventricular volumes, and in contrast to other studies, which showed, that ventricular dilation and thinning of the corpus callosum were the most frequent abnormalities on MRI^(84, 85) in preterm infants.

However, we have found that grade V of extension of the lateral ventricle exists only by preterm infants between 28 to < 32 weeks.

The existence of small porencephalic cysts (34%), which is known to be a form of a focal defect of cerebral substance due to localized cerebral insult in gestation, achieves its peak in our study at the mid-third trimester (32 to < 37 weeks).

The gradient-echo T2*-weighted MR image, which is quite sensitive to changes caused by blood breakdown products such as hemosiderin and ferritin⁽²⁷⁾, shows microbleeds in (11%) of our patients. All of them were premature at the early stage of third trimester 28 to < 32 gestational age, which could be related to the immaturity of vascular system at these groups of patients.

6. Conclusion:

In conclusion, this study has tried to find an easy quantitative marker in MRI, which might be applied by clinicians to predict the clinical outcome in children with BS-CP.

We have demonstrated quantitatively that the measurements of lateral ventricle, corpus callosum and midbrain are useful tools in determining the prognosis of CP. We did not find any evidence that gliosis, small porencephalic cysts or microbleeds are helpful in determining the severity of CP.

We determined the use of the depth of extraction of the lateral ventricle to distinguish between patients at GMFCS level I and IV, I and V and between II and V.

When the ratio of the length of the corpus callosum to the diameter of the skull by a patient with BS-CP is $\geq 0,34\%$, we can say with 95% CI that he could not have GMFCS V. When this ratio is lower than $0,33\%$ the patient had no GMFCS level I with 95% CI.

The quantitative assessment of the mean ratio of width of the posterior horn/ AP diameter of the skull allowed us with 95% CI to differentiate between GMFCS I ($0,08-0,12\%$) and IV ($0,14-0,19\%$).

The grade of extension of LV allowed us with 95% CI to differentiate between GMFCS levels I, II and GMFCS level IV.

However, other studies will be required to establish the validation and applicability of this method in a larger cohort of children with CP with brain lesions other than PWM.

Zusammenfassung

Das Ziel der Studie war es, einen einfach quantitativen Marker in der MRT zu identifizieren, der eine sichere Prognose bei Kindern mit BS-CP erlaubt.

Im Rahmen dieser quantitativen Studie konnten wir zeigen, dass die Messungen der lateralen Ventrikel, des Corpus callosum und des Mittelhirns sinnvolle Instrumente sind um die Prognose der CP einzuschätzen.

Das Vorliegen einer Gliose, porenzephaler Zysten oder Mikroblutungen waren dagegen nicht mit dem Schweregrad der CP assoziiert.

Des Weiteren untersuchten wir den Nutzen der Tiefe der Extraktion des lateralen Ventrikels mit Hinblick auf die Einstufung der Patienten in GMFCS I und IV, I und V und II und V.

Bei einem Verhältnis der Länge des Corpus callosum zu dem Durchmesser des Schädels von $\geq 0,34\%$, liegt mit einem 95% KI kein GMFCS V vor. Wenn dieses Verhältnis weniger als $0,33\%$ hat der Patient keine GMFCS I mit 95% KI.

Die quantitative Messung des Verhältnis von Breite des Hinterhorn zu AP Durchmesser des Schädels erlaubt uns mit 95% KI zwischen GMFCS I ($0,08-0,12\%$) und IV ($0,14-0,19\%$) zu unterscheiden.

Der Grad der Erweiterung der LV erlaubt uns, mit 95% KI zu unterscheiden zwischen GMFCS I, II und GMFCS IV.

Allerdings werden weitere Studien benötigt, Um die Validierung und Anwendbarkeit dieses Verfahren zu etablieren. Auch werden weiter Studien an größeren Gruppen von Kindern mit CP mit Gehirnläsionen anders als PWM benötigt.

7. References:

- 1 Himmelmann K., Hagberg G., Beckung E., Hagberg B., Uvebrant P. The changing panorama of cerebral palsy in Sweden. Prevalence and origin in the birth-year period 1995–1998, *Acta Paediatr*, 2005; 94 (3): 287–294
- 2 Asbury AK. et al, Cerebral palsy Diseases of the nervous system, Clinical neuroscience and therapeutic principles, *Cambridge University Press*, third edition, 2002: 568–580
- 3 Platt MJ., Cans C., Johnson A., Surman G., Topp M., Torrioli M.G., et al., Trends in cerebral palsy among infants of very low birthweight (<1500 g) or born prematurely (<32 weeks) in 16 European centres: a database study, *Lancet*, 2007; 369 (9555): 43–50
- 4 Robertson CM., Watt MJ., Yasui Y, Changes in the prevalence of cerebral palsy for children born very prematurely within a population-based program over 30 years, *JAMA*, 2007; 297 (24): 2733–2740
- 5 Ashwal S., Russman BS., Blasco PA., Miller G., Sandler A., Shevell M. et al., Practice parameter: diagnostic assessment of the child with cerebral palsy: report of the Quality Standards Subcommittee of the American Academy of Neurology and the Practice Committee of the Child Neurology Society, *Neurology*, 2004; 62 (6):851–863
- 6 Hart AR., Whitby EW., Griffiths PD., Smith MF., Magnetic resonance imaging and developmental outcome following preterm birth: review of current evidence, *Dev Med Child Neurol*, 2008; 50 (9):655–663
- 7 Robinson MN., Peake LJ., Ditchfield MR., Reid SM., Lanigan A., Reddiough DS., Magnetic resonance imaging findings in a population-based cohort of children with cerebral palsy, *Dev Med Child Neurol*, 2008; 51 (1): 39–45
- 8 Krägeloh-Mann I. Imaging of early brain injury and cortical plasticity. *Experimental Neurology*, 2004; 190 (1): 84–90
- 9 Heinen F. et al. The updated European Consensus 2009 on the use of Botulinum toxin for children with cerebral palsy. *Eur J Paediatr Neurol*. 2010; 14(1): 45-66
- 10 Bax M. et al, Proposed definition and classification of cerebral palsy, *Developmental Medicine & Child Neurology*, 2005; 47(8): 571- 576
- 11 Cans C. et al, Surveillance of cerebral palsy in Europe: a collaboration of cerebral palsy surveys and registers, *Developmental Medicine & Child Neurology*, 2000; 42 (12): 816-824
- 12 Krägeloh-Mann et al, Bilateral spastic cerebral palsy: A comparative study between southwest Germany and western Sweden. I: Clinical Patterns and disabilities, *Developmental Medicine & Child Neurol*, 1993; 35 (12): 1037–1047
- 13 Franz F., Reinhold K., Gudrun R., Gertrude K., Peter K., Reinhold S., Hans-Peter H., Histopathologic Analysis of Foci of Signal Loss on Gradient-Echo T2*-Weighted MR Images in Patients with Spontaneous Intracerebral Hemorrhage: Evidence of Microangiopathy-Related Microbleeds, *AJNR*, 1999; 20(4): 637– 642
- 14 Harvey SS., Jonathan W. M., Donald LG., Joseph J.. Movement Disorders in Childhood, *Elsevier Health Sciences*, 2010 Saunders; 5 (17): 219-230
- 15 Mutch L., Alberman E., Hagberg B. et al. Cerebral palsy epidemiology: where are we now and where are we going? *Dev Med Child Neurol*, 1992; 34(6): 547-551
- 16 Nelson KB. The epidemiology of cerebral palsy in term infants. *Ment Retard Dev Disabil Res Rev*, 2002; 8 (3):146–150
- 17 Miller G., Clark GD., The Cerebral Palsies: Causes, Consequences, and Management. Boston: Butterworth-Heinemann, 1998; 20 (5): 388-389
- 18 O'Shea TM: Cerebral palsy in very preterm infants: new epidemiological insights, *Ment Retard Dev Disabil Res Rev*, 2002; 8(3):135–145
- 19 Capute AJ.: Identifying cerebral palsy in infancy through study of primitive reflex profiles, *Pediatr Ann*, 1979; 8(10): 589–595
- 20 Keogh JM., Badawi N.: The origins of cerebral palsy. *Curr Opin Neurol*, 2006; 19(2):129–134
- 21 Capute AJ., Palmer FB., Shapiro BK., Wachtel RC., Ross A., Accardo PJ. Primitive reflex profile: a quantitation of primitive reflexes in infancy. *Dev Med Child Neurol*, 1984; 26(3):375-383
- 22 Gainsborough M., Surman G., Maestri G., et al. Validity and reliability of the guidelines of the surveillance of cerebral palsy in Europe for the classification of cerebral palsy. *Dev Med Child Neurol*, 2008; 50(11): 828-31
- 23 Beckung E., Hagberg G., Correlation between ICIDH handicap code and Gross Motor Function Classification System in children with cerebral palsy, *Developmental Medicine & Child Neurology*, 2000; 42 (10): 669–673
- 24 Krägeloh- Mann I. et al, Cerebral palsy update, *Brain and Development*, 2009; (31) 7: 537–544

- 25 Carnahan K., Arner M., Häggglund G., Association between gross motor function (GMFCS) and manual ability (MACS) in children with cerebral palsy. A population-based study of 359 children, *BMC Musculoskeletal Disorders*, 2007; 8:50
- 26 Wood E. The Gross Motor Function Classification System for Cerebral Palsy: a study of reliability and stability over time. *Developmental Medicine & Child Neurology*, 2000; 42(5): 292–296
- 27 Gage JR, Schwartz MH, Koop SE, The identification and treatment of gait problems in cerebral palsy. *Clinics in Developmental Medicine*, 2009; 180-181, 2 (1): 152
- 28 Ertl-Wagner B., Pädiatrische Neuroradiologie: Hypoxisch-ischämische Läsionen im Kindesalter, *Springer*, 2007; 7 (3): 149-154
- 29 Armstrong D., Halliday W., Hawkins C., Takashima S., Pediatric Neuropathology, *Springer*, 2007: 4 (2), 86- 88
- 30 Graham DI., Lantos PL., Greenfield' s neuropathology, Toxic and metabolic damage, white matter lesion. Periventricular leucomalacia, *Hodder Arnold Publication sixth edition*, 1997; 552-553
- 31 Panteliadis CP., Strassburg HM.: Cerebral Palsy: Principles and Management, Neuropathology of cerebral palsy, *Thieme Verlag*, 2004; 49-59
- 32 Golden JA., Harding BN., Developmental Neuropathology. White matter lesions in the perinatal period (20), *The International Society of Neuropathology*, 2004
- 33 Palisano RJ., Cameron D., Rosenbaum PL., Walter SD., Russell D., Stability of the gross motor function classification system. *Dev Med Child Neurol*, 2006; 48(6): 424-8
- 34 Palisano RJ, Hanna SE, Rosenbaum PL, Russell DJ, Walter SD, Wood EP, et al. Validation of a model of gross motor function for children with cerebral palsy. *Phys Ther*. 2000; 80(10):974-85
- 35 Palisano RJ, Rosenbaum P, Bartlett D, Livingston MH. Content validity of the expanded and revised Gross Motor Function Classification System. *Dev Med Child Neurol*. 2008; 50(10): 744-50
- 36 Forsyth R, Newton R. Pediatric Neurology, Cerebral Palsy, *Oxford university press*, 2012; 4: 227-243
- 37 Perlman JM., White matter injury in the preterm infant: an important determination of abnormal neurodevelopment outcome. *Early Human Development*, 1998; 53 (2): 99–120
- 38 Barkovich JA., Pediatric Neuroimaging, Brain and Spine Injuries in Infancy and Childhood, 5th Edition, *Lippincott Williams & Wilkins*, 2012; 272-277
- 39 Melhem ER., Hoon AH., Ferrucci JT, Quinn CB., Reinhardt EM., Demetrides SW., et al. Periventricular leukomalacia: relationship between lateral ventricular volume on brain MR images and severity of cognitive and motor impairment. *Radiology*. 2000; 214(1):199-204
- 40 Serdaroglu G., Tekgul H., Kitis O., Serdaroglu E., Gokben S., Correlative value of magnetic resonance imaging for neurodevelopmental outcome in periventricular leukomalacia. *Dev Med Child Neurol*. 2004; 46(11):733-9
- 41 Panigrahy A., Barnes PD., Robertson RL. , Sleeper LA., Sayre JW.. Quantitative analysis of the corpus callosum in children with cerebral palsy and developmental delay: correlation with cerebral white matter. *Pediatr Radiol*, 2005; 35(12): 1199–1207
- 42 Cioni G., Bertuccelli B., Boldrini A., Canapicchi R., Fazzi B., Guzzetta A., Mercuri E., Correlation between visual function, neurodevelopmental outcome, and magnetic resonance imaging findings in infants with periventricular leucomalacia. *Arch Dis Child Fetal Neonatal*. 2000, 82(2): 134–140
- 43 Fukuda S., Yokoi K., Suzuki S., Goto H.: Serial ultrasonographic observation of bilateral thalami in low birth weight infants with periventricular leukomalacia, *Brain Dev*, 2011; 33 (5): 394–399
- 44 Palmer SL., Reddick WE., Glass JO., Gajjar A., Goloubeva O., Mulhern RK.. Decline in Corpus Callosum Volume among Pediatric Patients with Medulloblastoma: Longitudinal MR Imaging Study. *AJNR*, 2002; 23 (7):1088–1094
- 45 Berne MR., Levy NM., Principles of Physiology, *Mosby*, 4th edition, 2000:140
- 46 Zach T., Pediatric Periventricular Leucomalacia Treatment & Management, *emedicine.medscape*, 2012
- 47 Volpe JJ, Brain injury in premature infants: a complex amalgam of destructive and developmental disturbances, *Lancet Neurology*, 2009; 8(1):110–124
- 48 Zou KH., Tuncali K., Silvermann SG., Correlation and Simple Linear Regression, *Radiology*, 2003; 227:617– 622
- 49 Hashimoto K., Hasegawa H., Kida Y., Takeuchi Y.: Correlation between neuroimaging and neurological outcome in periventricular leukomalacia: Diagnostic criteria, *Pediatrics International*, 2001; 43(3):240–245
- 50 Himmelmann K., Beckung E., Hagberg G., Uvebrant P., Bilateral spastic cerebral palsy: prevalence through four decades, motor function and growth. *Eur J Paediatr Neurol*. 2007; 11(4):215-222
- 51 De Vries LS et al, Correlation between the Degree of Periventricular Leucomalacia Diagnosed using Cranial Ultrasound and MRI, Later in Infancy in Children with Cerebral Palsy, *Neuropediatrics*, 1993; 24(5):

- 52 Serdaroglu G., Tekgul H., Kitis O., Sarenur G., Correlative value of magnetic resonance imaging for neurodevelopmental outcome in periventricular leukomalacia, *Developmental Medicine & Child Neurology*, 2004; 46(11): 733–739
- 53 Johnson A., Prevalence and characteristics of children with cerebral palsy in Europe, *Dev Med Child Neurol*. 2002; 44(9):633-40
- 54 Volpe JJ., Zipurksy, A., Neurobiology of Periventricular Leukomalacia in the Premature Infant, *Pediatric Research*, 2001; 50(5): 553–562
- 55 Inder TE., Huppi PS., Warfield S., Kikinis R., Zientara GP., Barnes PD., Jolesz F., Volpe JJ., Periventricular white matter injury in the premature infant is followed by reduced cerebral cortical gray matter volume at term, *Ann Neurol*, 1999; 46(5):755-60
- 56 Yoshida S., Hayakawa K., Yamamoto A., Kandab T., Yamori Y., Pontine Hypoplasia in Children with Periventricular Leukomalacia, *AJNR Am J Neuroradiology*, 2008, 29 (3):425-30
- 57 Argyropoulou et al, MRI measurements of the pons and cerebellum in children born preterm, associations with the severity of periventricular leukomalacia and perinatal risk factors, *Neuroradiology*, 2003;45(10):730–734
- 58 Yousem DM., Zimmerman RD., Grossman RI., *Neuroradiology: The Requisites*, 2nd ed. *Elsevier*, 2003, 55-66
- 59 Hayakawa K., Kanda T., Hashimoto K., Okuno Y., Yamori Y., Yuge M., Ando R., Ozaki N., Tamamoto A., MR imaging of spastic diplegia. The importance of corpus callosum, *Acta Radiol*, 1996; 37(5):830-6 sehr interessant
- 60 Wahl M., Lauterbach-Soon B., Hattingen E., Jung P., Singer O., Volz S., Klein JC., Steinmetz H., Ziemann U., Human Motor Corpus Callosum: Topography, Somatotopy, and Link between Microstructure and Function, *the Journal of Neuroscience*, 2007; 27(45):12132–12138
- 61 Hofer S., Frahm J., Topography of the human corpus callosum revisited—Comprehensive fiber tractography using diffusion tensor magnetic resonance imaging, *NeuroImage*, 2006; 32: 989–994
- 62 Barkovich AJ, Norman D., Anomalies of the Corpus Callosum: Correlation with Further Anomalies of the Brain, *AJR*, 1988; 151(1):493-501
- 63 Deng W., Pleasure J., Pleasure D., Progress in Periventricular Leukomalacia, *Arch Neurol*. 2008; 65(10):1291-1295
- 64 Lama S, Qiao M., Kirton A, Sun S., Cheng E., Foniok T., Tuor UI., Imaging Corticospinal Degeneration in Neonatal Rats with Unilateral Cerebral Infarction, *Experimental Neurology*, 2011; 228 (2): 192–199
- 65 Papadelis C., Leonardelli E., Staudt M., Braun C., Can magnetoencephalography track the afferent information flow along white matter thalamo-cortical fibers? *Neuroimage*, 2012; 60(2): 1092–1105
- 66 Kuhn MJ., Mikulis DJ., Ayoub DM., Kosofsky BE., Davis KR., Taveras JM., Wallerian degeneration after cerebral infarction: Evaluation with sequential MR imaging, *Radiology*, 1989; 172 (1): 179–182
- 67 Domi T., DeVeber G., Shroff M., Kouzmitcheva E., MacGregor D.L., Kirton A. Corticospinal Tract Pre-Wallerian Degeneration: A Novel Outcome Predictor for Pediatric Stroke on Acute MRI Stroke, *Stroke*, 2009; 40 (3): 780–787
- 68 Maunu J., Lehtonen L., Lapinleimu H., Matom J., Munck P., Ventricular dilatation in relation to outcome at 2 years of age in very preterm infants: a prospective Finnish cohort study, *Developmental Medicine & Child Neurology*, 2011; 53(1): 48–54
- 69 Jeon TY. et al, Neurodevelopmental outcomes in preterm infants: comparison of infants with and without diffuse excessive high signal intensity on MR images at near-term-equivalent age, *Radiology*, 2012; 263(2): 518-526
- 70 Francisca T.de Bruine et al, Clinical Implications of MR Imaging Findings in the White Matter in Very Preterm Infants: A 2-year Follow-up Study, *Radiology*, 2011; 261(3): 899-906
- 71 Skranes J. et al, Abnormal cerebral MRI findings and neuroimpairments in very low birth weight (VLBW) adolescents, *European Journal of paediatric neurology*, 2008;12(4): 273–283
- 72 Ment LR., Vohr B., Walter A., Westerveld M., Katz KH., Schneider K. Makuch RW., The Etiology and Outcome of Cerebral Ventriculomegaly at Term in Very Low Birth Weight Preterm Infants, *Pediatrics*, 1999; 104, 243
- 73 Skranes J, Martinussen M, Smevik O, et al. Cerebral MRI findings in very-low-birth-weight and small-for-gestational age children at 15 years of age. *Pediatr Radiol*, 2005; 35:758–65
- 74 Fedrizzi E., Inverno M., Bruzzone MG., Botteon G., Saletti V., Farinotti M. MRI features of cerebral lesions and cognitive functions in preterm spastic diplegic children. *Pediatr Neurol*, 1996; 15(3):207-212
- 75 Wojciech et al, Spastic cerebral palsy: clinical magnetic resonance imaging correlation of 129 children. *J Child Neurol*. 2007; 22: 8-14.
- 76 Kwong KL., Wong YC., Fong CM., Wong SN., Magnetic resonance imaging in 122 children with spastic

cerebral palsy. *Pediatr Neurol*. 2004; 31(3):172-176

- 77 Okumura A., Kato T., Kuno K., et al. MRI findings in patients with spastic cerebral palsy II: correlation with type of cerebral palsy. *Dev Med Child Neurology*. 1997; 39(6), 369-372
- 78 Krägeloh-Mann I, Hagberg B, Petersen D, et al. Bilateral spastic cerebral palsy: MRI pathology and origin. Analysis from a representative series of 56 cases. *Dev Med Child Neurol*. 1995; 37(5):379-397
- 79 Okumura A., Hayakawa F., Kato T., Kuno K., Watanab K., MRI findings in patients with spastic cerebral palsy. I: correlation with gestational age at birth, *Developmental Medicine & Child Neurology*, 1997, 39(6): 363–368
- 80 Staudt M et al, Pyramidal tract damage correlates with motor dysfunction in bilateral periventricular leukomalacia (PVL). *Neuropediatrics*. 2003; 34(4):182-8
- 81 Angeles Fernández-Gil M., Palacios-Bote R., Leo-Barahona M., Mora-Encinas J.P., Anatomy of the Brainstem: A Gaze into the stem of life, *Elsevier*, 2010; 31(3):196-219
- 82 Bühl A. PASW 18: Einführung in die moderne Datenanalyse ; [ehemals SPSS], aktualisierte Aufl. ed. München [u.a.]: Pearson Studium, 2010
- 83 Yin R et al, Magnetic resonance imaging findings in cerebral palsy, *J. Paediatr Child Health* (2000) 36 (2), 139-144
- 84 Stewart A, Kirkbride V, Very preterm infants at fourteen years: relationship with neonatal ultrasound brainscans and neurodevelopmental status at one year. *Acta Paediatr*, 1996; 85 (416): 44–47
- 85 Stewart A, Rifkin L, Amess PN et al, Brain structure and neurocognitive and behavioural function in adolescents who were born very preterm. *Lancet*, 1999, 353: 1653–1657
- 86 Gordon CS S. et al, Maternal and biochemical predictors of spontaneous preterm birth among nulliparous women: a systematic analysis in relation to the degree of prematurity, *International Journal of Epidemiology* 2006;35:1169–1177
- 87 Loukia C. et al, Periventricular leukomalacia in preterm children: assessment of grey and white matter and cerebrospinal fluid changes by MRI, *Pediatr Radiol*, January 2009, 39(12): 1327-1332
- 88 Burad L. Et al, Recognition and management of fetal alcohol syndrome, *Neurotoxicology and teratology*, December 2003, 25(6): 681–688
- 89 Blencowe H, Cousens S, Oestergaard M, Chou D, Moller AB, Narwal R, Adler A, Garcia CV, Rohde S, Say L, Lawn JE. National, regional and worldwide estimates of preterm birth. *The Lancet*, June 2012. 9;379(9832):2162-72. Estimates from 2010.
- 90 Van Haastert et al, Decreasing Incidence and Severity of Cerebral Palsy in Prematurely Born Children, *Journal of Pediatrics*, (in press) DOI: 10.1016/j.jpeds2010.12.053
- 91 Barkovich AJ, Kjos BO. Normal Postnatal Development of the Corpus Callosum as Demonstrated by MR Imaging. *AJNR*. 1988;9:487-491.
- 92 Fiori S, Cioni G, Klingels K, Ortibus E, Van Gestel L, Rose S, Boyd RN, Feys H, Guzzetta A. Reliability of a novel, semiquantitative scale for classification of structural brain magnetic resonance imaging in children with cerebral palsy. *Developmental Medicine & Child Neurology*. September 2014; 56 (9): 839–845.
- 93 Kazunari et al, Clinical impact of the callosal angle in the diagnosis of idiopathic normal pressure hydrocephalus, *Eur Radiol* (2008) 18:2678–2683
- 94 Krageloh-Mann, V. Horber. The role of magnetic resonance imaging in elucidating the pathogenesis of cerebral palsy: a systematic review. *Dev. Med. Child Neurol.*, 49 (2) (2007), pp. 144–151
- 95 Parazzini C, Baldoli C, Scotti G, Triulzi F. Terminal zones of myelination: MR evaluation of children aged 20–40 months. *AJNR Am J Neuroradiol* 2002; 23: 1669–73

8. List of figures

FIG.1	Gross motor curves	14
FIG.2	Periventricular leukomalacia (PVL) the multiple white spots (necrotic foci) in periventricular white matter	15
FIG.3	Macroscopic appearance of the PVL lesions	16
FIG.4	Periventricular leukomalacia, dilated ventricles and reduced white matter volume	16
FIG.5	PVL Coronal section of the cerebrum. The two components of the lesion, deep focal areas of cystic necrosis and more diffuse cerebral white matter injury	16
FIG.6	Multicystic leukomalacia present in the brain of neonate at the time of death, marked destruction of the white matter	17
FIG.7	The motor tract	18
FIG.8	Coronal ultrasound view from preterm infant with PVL	19
FIG.9	a: MRI axial flair, increased signal intensity in the periventricular white matter b: MRI axial flair, the lateral ventricles are extended and atypical configured c: MRI flair axial, the ventricular enlargement with irregular outline of the lateral ventricles d: MRI sagittal T1-weighted, the thinning of the corpus callosum and the reduced quantity of white matter	20
FIG.10	Midsagittal T2-weighted image, MRI-parameters	26
FIG.11	Axial T1-weighted images, MRI-parameters diameter of the cerebral peduncles and diameter of the midbrain axial	26
FIG.12	Axial T2-weighted MR images, the optic classification of the extension of lateral ventricle	26
FIG.13	Axial T2-weighted MRI, width of the posterior horn of the lateral ventricle, distance between the lateral ventricles and the cortex, distance between the lateral extraction of the ventricles and the cortex, deep of lateral extraction of lateral ventricles	27
FIG.14	Axial flair MRI, optic classification of the grade of the gliosis	27
FIG.15	Axial flair MRI, width of the gliosis and distance between the gliosis and the cortex	28
FIG.16	Axial flair, a: small porencephalic cyst. b: axial T2*-Weighted GER deposits of microhemorrhages in PVL	28
FIG.17	Witelson's scheme, Corpus callosum subregions	28
FIG.18	Transcallosal fiber tracts	28
FIG.19	Flow diagram for determination of patients' collective	31
FIG.20	Distribution of patients according to GMFCS	31
FIG.21	Box plot of patients according to GMFCS by gestational age	32
FIG.22	Distribution of severity of GMFCS according to groups of gestational age	32
FIG.23	Ratio of length of corpus callosum (95% CI) by GMFCS	34
FIG.24	Ratio of thickness of the genu to the AP diameter of skull (95% CI) by GMFCS	35

FIG.25	MRI mid-sagittal T1-weighted. Correlation between the corpus callosum and the severity of cerebral palsy according to GMFCS	36
FIG.26	Ratio of thickness of thinnest part of corpus callosum (95% CI) by GMFCS	36
FIG.27	Distribution of location of thinnest part of corpus callosum	37
FIG.28	Distribution of location of thinnest part of corpus callosum by patients with CP according to GMFCS	37
FIG.29	Scatter plot of length of corpus callosum and thickness of thinnest part of of corpus callosum, thickness of genu and length of corpus callosum, thickness of thinnest part of corpus callosum and thickness of genu	38
FIG.30	MRI show location of thinnest part of corpus callosum	39
FIG.31	Mean ratio of diameter of midbrain axial to AP diameter of skull X 10 by GMFCS (95% CI)	41
FIG.32	Mean ratio of diameter of midbrain sagittal to AP diameter of skull X 10 by GMFCS (95% CI)	41
FIG.33	MRI T1-sagittal show the atrophy of midbrain according to GMFCS	41
FIG.34	Mean ratio of axial diameter of cerebral peduncles to AP diameter of skull (95% CI) by GMFCS	42
FIG.35	Mean ratio of craniocaudal diameter of pons axial to AP diameter of skull by GMFCS (95% CI)	43
FIG.36	Distribution of grade of extension of LV according to severity of CP	44
FIG.37	Mean grade of extension of lateral ventricle (95% CI) by GMFCS	44
FIG.38	Mean ratio of width of posterior horn of the lateral ventricle to AP diameter of skull (95% CI) by GMFCS	45
FIG.39	Mean depth of extraction of lateral ventricle (95%CI) by GMFCS	46
FIG.40	Mean distance between lateral ventricle and cortex (95% CI) by GMFCS	47
FIG.41	Distance between extraction of lateral ventricle and cortex by GMFCS (95% CI)	47
FIG.42	Distribution of grade of gliosis according to severity of CP	48
FIG.43	Width of gliosis by GMFCS (95% CI)	49
FIG.44	Mean distance between gliosis and cortex (95% CI) by GMFCS	50
FIG.45	Existence of small porencephalic cysts in our study	51
FIG.46	Distribution of small porencephalic cysts according to GMFCS	51
FIG.47	Existence of microhemorrhages on T2*-weighted gradient echo MR in our study	52
FIG.48	Existence of microhemorrhages on T2*-weighted gradient echo MR according to severity of cerebral palsy	52
FIG.49	Scatter plots show correlation between right and left-findings on MRI	52
FIG.50	Distribution of patients according to gestational age	53

9. List of tables:

Tab.1	Pattern of brain lesions relative to the stage of brain development	10
Tab.2	Classification of cerebral palsy	11
Tab.3	Gross Motor Function Classification System (GMFCS) Levels 1-5 at age 6-12 years	13
Tab.4	Clinical Data of the patients in our study	23
Tab.5	Groups of patients according to gestational age at delivery	23
Tab.6	MRI-parameters which were measured in our study	24
Tab.7	Correlation between the variables	29
Tab.8	Interpretation of Correlation Coefficient	29
Tab.9	Descriptive statistic of patients in our study	30
Tab.10	Correlation between the following variables and gestational age and GMFCS according to Pearson's rank correlation	30
Tab.11	Distribution of patients according to type of CP by GMFCS	32
Tab.12	Descriptive statistical of age at the time of MRI by GMFCS	33
Tab.13	Descriptive statistic of severity of cerebral palsy by length of corpus callosum	33
Tab.14	Descriptive statistic of severity of cerebral palsy by thickness of genu	34
Tab.15	Descriptive statistic of GMFCS by thickness of thinnest part of corpus callosum	35
Tab.16	Location of the thinnest part of CC in patients with CP	37
Tab.17	Descriptive statistic of the ratio of axial diameter of midbrain(mm) /anterior-posterior diameter of the skull (mm) X10 by GMFCS	40
Tab.18	Descriptive statistic of the ratio of sagittal diameter of midbrain(mm) /anterior- posterior diameter of skull (mm) X10 by GMFCS	40
Tab.19	Descriptive statistic of the ratio of axial diameter of cerebral peduncles (mm)/ AP diameter of the skull (mm) by GMFCS	42
Tab.20	Descriptive statistic of the ratio of craniocaudal diameter of the pons (mm) to AP diameter of the skull (mm) by GMFCS	43
Tab.21	Descriptive statistic of grade of extension of the lateral ventricle by GMFCS	44
Tab.22	Descriptive statistic of the ratio of width of posterior horn of the lateral ventricle to AP diameter of the skull by GMFCS	45
Tab.23	Descriptive statistic of depth of extraction of the lateral ventricle by GMFCS level	46
Tab.24	Descriptive statistic of distance between lateral ventricle and cortex by GMFCS	46
Tab.25	Descriptive statistic of distance between extraction of the lateral ventricle by GMFCS	47
Tab.26	Descriptive statistic of grade of gliosis by GMFCS	48
Tab.27	Descriptive statistic of width of gliosis on both sides by GMFCS	49
Tab.28	Descriptive statistic of distance between gliosis and cortex by GMFCS	50
Tab.29	Descriptive statistic of existence of small porencephalic cysts on MRI by GMFCS	51

Tab.30	Descriptive statistic of existence of microhemorrhages on T2*-Weighted MRI by GMFCS	51
Tab.31	Correlation between right and left-findings on MRI	52
Tab.32	Correlation between Gestational age and MRI-findings	55

10. Abbreviations:

AP	Anterior posterior
BS-CP	Bilateral spastic cerebral palsy
CBF	Cerebral blood flow
CC	Corpus Callosum
CNS	Central nervous system
CP	Cerebral palsy
CSF	Cerebrospinal fluid
DGP	Dyskinetic cerebral palsy
et al.	et alii (and others)
e.g.,	For example
FIG	Figure
GA	Gestational age
GER	Gradient Echo Sequence
GMFCS	Gross Motor Function Classification System
i.e.	Id est
LV	Lateral ventricles
Max.	Maximal
MBP	Myelin basic protein
Min	Minimal
MRI	Magnetic Resonance Imaging
N	Number
OL	Oligodendroglia
PVL	Periventricular leukomalacia
PVWM	Periventricular white matter
SD	Standard deviation
Tab	Table
TNF	Tumor necrosis factor
USCP	Unilateral spastic cerebral palsy
VLBW	Very low birth weight
VP-Shunt	Ventriculoperitoneal shunt
VS	Versus
WGA	Weeks of gestational age
WM	White matter
Yrs	Years

11. Appendix:

Overview of all patients in our study																												
ID	AP Skull I	Mid brain axial	Cereb ral pedu ncle axial left	Cereb ral pedu ncle axial right	Pons sag.	Mid brain sag.	LV- exten sion	Width of posterior horn LV L	Width of posterior horn LV (R)	Depth of extrac tion of LV (L)	Cortex- extract ion of LV (L)	Cortex - extract ion of LV (R)	LV - cortex x (L)	LV - cortex x (R)	Glios grade 1 to 5	Width of gliosis (L)	Width of gliosis (R)	Glios - cortex (L)	Glios - cortex (R)	Length of CC	Thickn ess of genu	Thickn ess of thinne st part of CC	GMFCS	Small porence phalic cyst	Micro- haemo rrhage	Artefa cts		
70	16	12	12	12	21	11	1	6	9	,0	,0	,0	,0	3,0	3,0	2	7	6	2,5	2,5	6	2,5	8	1	0	0	1	
91	18	11	13	14	27	12	1	7	5	,0	,0	,0	,0	2,5	2,5	2	5	5	2,0	2,0	6	2,5	9	1	0	0	1	
32	17	14	12	12	22	12	1	7	10	,0	,0	,0	,0	3,0	2,0	4	12	12	1,0	1,0	6	1,5	8	1	1	0	1	
61	22	15	17	15	25	15	1	9	11	2,5	1,5	9,0	9,0	3,0	3,0	4	15	11	,0	,0	7	3,0	10	1	1	0	1	
2	16	17	2	12	12	2,2	1,5	6,0	10,0	3,0	3,0	4	13	13	2,0	2,5	6	1,5	9	1	1	0	4	
25	17	16	14	13	20	.	2	16	9	2,0	1,0	9,5	8,0	3,0	2,0	3	6	7	1,5	2,0	7	3,0	10	1	0	0	1	
95	20	15	14	14	25	12	2	12	6	2,5	1,5	5,0	7,0	2,0	2,0	2	5	5	1,5	1,5	6	2,0	13	1	0	.	1	
35	18	14	14	15	27	11	3	13	13	2,5	,5	5,5	4,5	2,0	2,0	2	5	4	1,0	2,0	7	3,0	10	1	0	0	2	
49	17	13	13	13	22	13	1	6	5	,0	,0	,0	,0	6,5	6,5	3	2	11	18,0	2,5	6	3,0	11	1	0	.	1	
78	16	11	12	12	19	11	1	6	5	,0	,0	,0	,0	4,0	3,0	2	6	6	2,0	2,5	5	2,0	9	1	0	0	1	
93	18	11	14	13	21	10	1	11	8	,0	,0	,0	,0	3,5	3,5	2	4	4	5,0	5,0	6	2,0	10	1	0	0	1	
79	16	12	12	11	19	11	2	13	10	1,5	,5	5,0	4,0	4,0	3,0	2	5	4	3,0	3,0	6	3,0	10	1	0	0	1	
4	19	15	2	13	6	2,5	1,0	15,0	10,0	2,5	2,5	2	6	3	4,0	3,0	7	3,0	9	1	0	0	1	
28	17	13	12	11	20	.	1	9	9	1,0	1,0	7,0	6,0	3,0	3,0	3	8	8	2,0	2,0	6	3,0	7	2	0	0	1	
57	20	15	14	13	25	12	1	6	7	,0	,0	,0	,0	,0	,0	5	10	14	,0	,0	6	,5	2	2	1	0	1	
68	16	11	10	10	20	10	1	4	4	2,0	1,0	7,0	5,0	2,0	2,0	4	10	10	1,5	1,5	5	1,5	8	2	0	0	1	
81	16	11	11	11	23	10	1	7	7	1,0	1,0	3,0	6,0	,0	,0	5	16	17	,0	,0	5	1,0	7	2	1	0	1	
14	17	13	2	13	14	,0	,0	,0	,0	2,5	2,5	2	7	7	1,5	1,5	6	1,0	8	2	0	0	1	
34	16	15	13	12	23	10	3	16	16	2,5	4,5	4,0	2,0	,0	,0	4	11	18	,0	,0	5	2,0	8	2	1	0	2	
26	18	14	13	12	21	.	1	9	6	1,0	1,0	5,5	4,5	2,5	2,5	4	11	10	2,5	2,0	6	1,5	8	2	1	0	1	
73	16	11	11	11	19	10	1	6	7	,5	,5	3,0	4,5	3,0	3,0	3	9	10	3,0	3,0	6	2,0	7	2	0	0	1	
3	16	12	2	12	12	1,0	,0	11,0	11,0	3,0	3,0	2	6	6	5,0	5,0	6	4,5	9	2	0	0	1	
20	19	16	14	14	25	.	2	12	14	1,5	1,5	5,0	6,0	3,0	3,0	2	7	7	2,0	1,0	7	3,5	10	2	0	0	2	
82	18	10	10	12	21	10	3	13	14	2,0	1,5	,0	,0	,0	,0	4	13	13	,0	,0	5	1,5	3	2	1	0	1	
76	18	13	13	12	22	11	3	12	13	3,5	3,5	7,5	7,0	2,0	1,0	3	6	6	,5	,5	7	2,5	12	2	0	0	1	
55	16	10	12	12	21	9	2	11	11	1,0	1,0	6,0	7,0	1,0	1,0	3	6	6	1,0	1,0	6	2,0	9	2	0	0	1	
33	17	13	12	12	19	11	3	16	12	1,0	1,0	3,0	,0	,0	,0	4	12	10	,0	,0	5	1,0	6	3	0	0	1	
47	16	12	11	12	21	9	4	16	13	2,5	2,5	6,5	7,5	3,0	4,0	2	5	5	3,0	3,0	6	2,0	9	3	0	0	1	
30	18	16	15	15	25	.	1	9	5	2,5	2,5	3,5	4,0	1,5	1,0	2	8	7	1,5	1,0	6	1,5	11	3	0	0	1	
77	16	12	11	12	21	11	1	8	9	2,5	1,5	.	1,5	1,0	1,0	4	9	10	1,0	1,0	5	2,0	10	3	0	0	1	
53	16	12	11	10	18	10	2	12	8	2,0	1,0	4,0	5,0	1,0	1,0	3	6	7	2,0	2,0	5	2,5	8	3	0	0	1	
39	16	13	11	11	20	9	2	10	10	,5	,5	6,5	6,5	2,0	3,0	2	4	4	2,0	2,0	6	1,0	7	3	0	0	1	
62	17	12	12	12	20	12	2	10	12	3,0	3,0	7,0	6,0	1,5	1,0	3	7	7	1,5	1,5	6	2,5	9	3	1	0	1	
21	20	14	17	16	24	.	2	14	12	2,5	1,5	2,5	2,0	1,0	1,0	2	6	6	1,0	1,0	7	1,5	11	3	0	0	2	
16	15	13	11	11	17	.	3	14	14	2,0	2,0	14,0	11,0	3,5	3,0	2	5	5	1,5	1,5	6	1,5	8	3	0	0	1	
74	18	11	11	11	20	10	4	23	15	2,5	2,5	3,0	3,0	1,0	1,0	3	10	10	1,0	1,0	7	1,0	7	3	0	1	1	
58	17	13	11	10	19	9	2	10	10	1,5	1,5	3,0	3,0	,5	,0	3	9	7	1,5	1,5	5	2,0	7	3	0	0	1	
52	16	12	10	11	22	9	2	14	11	,0	,0	,0	,0	,0	,0	5	13	13	,0	,0	5	1,0	3	4	1	0	1	
98	16	9	10	10	18	10	4	13	12	2,0	2,0	3,0	4,0	,0	,0	5	15	14	,0	,0	4	1,0	3	4	0	0	1	
29	16	14	12	12	25	.	2	10	10	3,0	2,0	4,5	4,5	1,0	1,0	4	9	11	1,0	1,0	5	1,5	5	4	1	0	1	
44	16	12	11	11	20	9	2	9	10	2,0	2,5	2,0	,5	,0	0	4	14	15	1,0	,5	5	1,0	7	4	1	0	1	
65	18	14	14	14	27	11	2	14	13	4,0	3,0	6,0	8,0	5,0	5,0	2	5	5	3,0	3,0	7	2,0	8	4	0	0	4	
24	17	12	10	11	21	.	3	16	14	3,0	1,5	2,0	3,0	,0	,0	4	13	12	,0	,0	5	1,0	5	4	1	0	1	
18	19	14	14	14	25	.	3	17	16	2,5	2,5	6,0	6,0	2,0	2,0	3	8	8	1,0	1,0	7	3,0	10	4	1	0	2	
92	17	13	12	12	19	8	4	11	11	4,5	4,0	4,0	3,0	,0	,0	3	7	6	,0	,0	5	2,0	9	4	1	0	1	
94	16	12	10	10	16	10	5	16	14	3,0	4,0	3,0	2,0	,0	,0	4	9	9	,0	,0	5	,5	2	4	1	1	1	
66	16	11	9	10	12	9	5	25	15	5,0	4,0	1,0	1,0	,0	,0	2	2	2	,0	,0	5	,5	1	4	0	1	1	
40	15	10	10	10	21	9	1	6	5	3,0	2,0	5,5	5,5	1,5	1,5	5	12	14	,0	,0	4	1,5	6	5	0	0	1	
46	19	13	12	12	21	11	2	10	10	3,5	1,5	5,0	6,0	1,0	,0	4	10	11	,0	,0	6	2,0	7	5	1	0	4	
36	18	9	10	10	18	10	5	22	22	2,5	3,0	4,0	4,0	,0	,0	2	3	3	,0	,0	5	,5	5	5	0	0	1	
Tot al	50	50	50	46	46	36	50	50	50	50	48	50	50	50	50	50	50	50	50	50	50	50	50	50	50	48	50	

12. Thanks

At the end of this study, I would like to say a lot of thanks for Prof. Heinen for the assignment for this theme. I was glad to learn from you Prof. Heinen.

I thank Prof. Ertl- Wagner for her excellent support.

Very special thanks for PD. Schröder for his kindness and support throughout this study. I thank you Sebastian for all and wish you the best for your future.

For my husband is special thanks for his help and encouragement.

Eidesstattliche Versicherung

Al Hallak, Maesa

Name, Vorname

Ich erkläre hiermit an Eides statt,

dass ich die vorliegende Dissertation mit dem Thema

Correlation between Gross Motor Function and MRI Brain Morphology in Children with Cerebral Palsy

selbständig verfasst, mich außer der angegebenen keiner weiteren Hilfsmittel bedient und alle Erkenntnisse, die aus dem Schrifttum ganz oder annähernd übernommen sind, als solche kenntlich gemacht und nach ihrer Herkunft unter Bezeichnung der Fundstelle einzeln nachgewiesen habe.

Ich erkläre des Weiteren, dass die hier vorgelegte Dissertation nicht in gleicher oder in ähnlicher Form bei einer anderen Stelle zur Erlangung eines akademischen Grades eingereicht wurde.

München, 08.06.2018

Ort, Datum

Maesa Al Hallak

Unterschrift Doktorandin/Doktorand